Simulation and Modelling of Solar Dryer in COMSOL: Analysis of Airflow

Thesis for the Degree of Master of Science in Electrical Engineering.

Division of Energy and Building Design. Department of Building and Environmental Technology

LUND UNIVERSITY

LTH

FACULTY OF ENGINEERING

Author: Christoffer Sörensson
Supervisor: Dr. Martin Anderssson
Examiner: Dr. Henrik Davidsson

Abstract

"Solar Food: Reducing post-harvest losses through improved solar drying" is a project that is a collaboration between Lund University and the Royal University of Bhutan, financed by the Swedish Research Council. The goal of the project is to improve the quality and decrease post-harvest losses of food in rural Bhutan and Nepal through low-cost, efficient solar-powered food dryers.

In this diploma project, the airflow of the two existing designs was evaluated by running simulations in the software COMSOL. The results of the simulations were then analyzed to come up with design changes to improve the airflow of the two solar dryers and suggest a new solar dryer design.

There are some flaws in the two existing designs, as both have the same issues when it comes to airflow. Each design has issues with a significant amount of air flowing along the wall in the first drying chamber, and with an air vortex forming in the second drying chamber that can lead to uneven drying. The issue with the air vortex in the second drying chamber may lie in the design of the centre panel and how it restricts the airflow between the two drying chambers, leading to an increase in air velocity which creates the air vortex. The adjustments, such as a larger entry gap to the drying chamber and changing the placement of the internal fan, made to the two designs that are simulated in this project did not solve these two mentioned problems and only provided small indications of improved airflow. However, the size of these improvements cannot be determined and more calculations needs to be done to confirm these improvements and the size of them.

The results from the simulations using a new design with one drying chamber have raised more questions than answers, and therefore there is no reason to continue working on this design or to conduct any experiments on it. Regarding the first and second designs, the first design seems to have fewer problems to solve when it comes to airflow. To determined which of the two designs are better, more experiments needs to be conducted on the two designs.

Contents

1 Introduction

1.1 Project Background and Goals

This report is part of an ongoing project, Solar Food: Reducing post-harvest losses through improved solar drying. The project is a collaboration between Lund University and the Royal University of Bhutan, and financed by the Swedish Research Council. The goal with the project is to improve the quality and decrease post-harvest losses of food in rural Bhutan and Nepal through low-cost efficient solar powered food dryers.

In this project, the two existing designs airflow was evaluated by running simulations in the software COMSOL. The results of the simulations were then analysed to come up with design changes to improve the airflow of the two solar dryers and suggest a new solar dryer design. The simulations were run with the following questions in mind:

- Are there any design flaws on the two existing designs when it comes to optimal airflow?
- Is it possible to make small adjustments on the two designs to improve the airflow inside the dryer?
- With focus on improving the airflow, how could a new design look like?

1.2 Project Introduction

Most types of food can only be harvested during certain seasons and this makes preservation important. Without preservation it is not possible to have a steady supply of food all year round. There are different kinds of food preservation methods, among the oldest are drying, and the purpose of all the different methods is to slow down the chemical and physical deterioration that occurs within the food (Desrosier & Singh, 2024). Doing this also gives the possibility to be able to transport the food longer distances, which is beneficial in mountainous areas where access is limited. Today in Bhutan, open-air food drying is regularly used due to its low cost and accessibility to farmers. Typically, farmers use their roofs to dry crops like ginger or chili fruits. However, this method lacks temperature control and leads to challenges in regulating the drying process. Consequently, there are high levels of post-harvest losses and variability in the quality of the finished product due to nutrient degradation from direct sunlight exposure (Ndawula, 2023). The reduced quality of the product results in lower selling prices, impacting the income of the 60% of the population that relies on farming for livelihoods (The World Bank, 2017). Additionally, Bhutan faces a unique challenge with 11.4% of Bhutanese being obese and 33.5% overweight, despite persistent micronutrient deficiencies being a major public health issue (WFP, 2020). Improving food preservation methods can help preserve nutrient content, increase efficiency, and reduce food losses and spoilage. These improvements aim to enhance overall food quality, support farmers in reducing waste, and potentially improve profitability within the agricultural sector.

2 Background

2.1 Bhutan

Bhutan is a country of south-central Asia, located in the eastern part of the Himalayas. The country can be divided into three different regions: the Great Himalayas, the Lesser Himalayas, and the Duars plain. These three regions have very different climates. In the northern part of the country, in the region of the Great Himalayas, there are mountain peaks with heights up to 7 300 metres and high valleys between 3 700 to 5 500 metres. This gives the region a dry climate (Karan et al., 2023). The Lesser Himalayas region also consists of mountains and valleys. But the peak heights vary from 1 500 to 2 700 metres, much lower than the Great Himalayas region. The valleys are relatively broad and flat. This region receives moderate rainfall of about 1 000 to 1 270 mm or less a year and the region is also well populated (Karan et al., 2023). The Duars plain is located south of the Lesser Himalayas, along the southern border of Bhutan. It is a narrow patch of land that is 12 km to 16 km wide. The Himalayan Mountain ranges rise abruptly from the Duars plain. This gives a tropical and humid climate in the region with rainfall around 5 100 to 7 600 mm a year (Karan et al., 2023).

2.1.1 Economics

Bhutan is a landlocked country; trade and transit arrangements with other countries play a critical role in Bhutan's economy. India is the largest source of imports and the largest destination for exports for Bhutan, and the countries have a free trade arrangement with each other (Karan et al., 2023). Bhutan has sustained an average GDP growth of 7.5 % since the 1980s, leading to a reduction in the number of people living in poverty. This growth has been driven by the public sector-led hydropower and services sectors, including tourism. Since the pandemic, tourism has still not fully recovered to pre-COVID levels, but the service sector still managed to grow by 5% during 2022. Despite the economic growth that Bhutan has experienced, around 7% of the population remains vulnerable to poverty (The World Bank, 2023), which can lead to issues such as food insecurity and malnutrition (The World Bank, 2017).

2.1.2 Agriculture

Agriculture in Bhutan employs 60% of Bhutan's population (The World Bank, 2017). Farming is limited by the mountain peaks and valleys, which also makes it more difficult. Contributing factors to this are the mountainous topography and rapid changes in weather. Climate change is also a contributing factor that makes farming even harder. Bhutan has already experienced crop loss due to climate change, with outbreaks of unusual diseases and pests, windstorms, hailstorms, erratic rainfall, droughts, flash floods, and landslides (Chhogyel & el al., 2018)..

2.2 Project-Food Dryer

2.2.1 First Design

The first design of the solar dryer to be simulated in this project is equipped with a heat exchanger, an absorber, heat storage, a drying chamber with six shelves, an internal fan, and an external fan; both fans are 12 V DC fans. Figure 1 shows the dryer, and the direction of airflow is also visualised in the figure with arrows. The colours of the arrows indicate air temperature, where blue represents colder air and red represents warmer air.

The dryer operates by drawing in air from the surroundings with the help of the external fan through a circular inlet. The air passes by the aluminium heat exchanger, then moves upwards towards the top of the dryer, where it passes by the aluminium absorber. The absorber has been heated by sunlight, which enters through the piece of glass on the top of the dryer, angled at 30°. Afterwards, the air descends into the drying chamber, where it is mixed with cooler, more humid recirculated air from the internal fan. Finally, the air passes along the other side of the heat exchanger before exiting through the outlet.

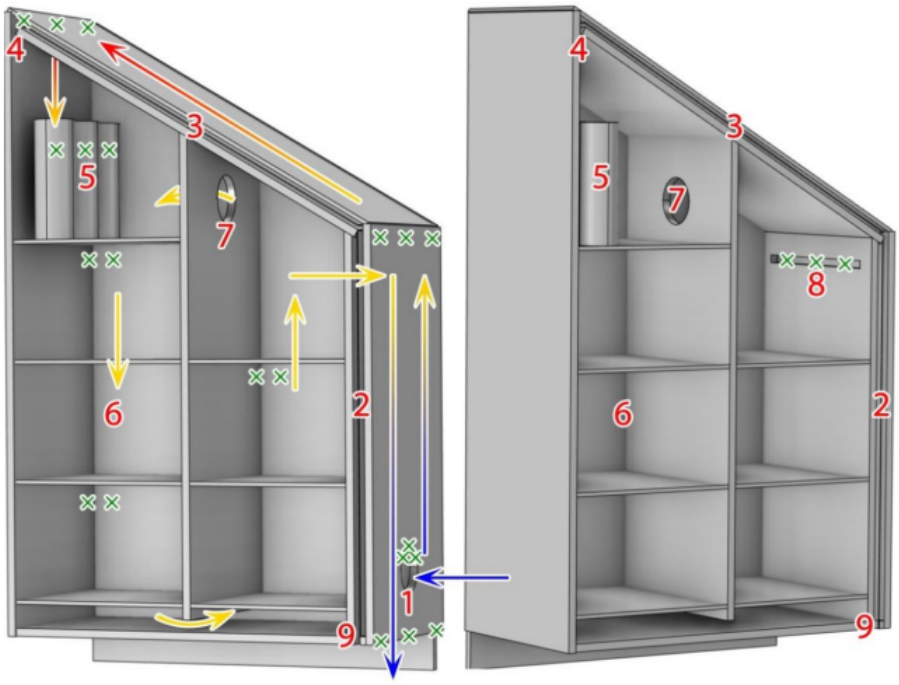

Figure 1: *The food dryer's 3D model is viewed from two distinct angles. In the picture, the numbered pieces include the following, which are arranged in sequential sequence based on the air flow through the dryer. 1. Dryer inlet; 2. Heat exchanger; 3. Absorber; 4. Absorber outlet; 5. Heat storage; 6. Drying chamber; 7. Internal fan; 8. Drying chamber outlet; 9. Dryer outlet. Each of the green crosses indicate the locationof one thermocouple, all displayed in the left image except for the three by the drying chamber outlet which are displayed in the right image. The arrows point in the direction of the air flow while the colour indicates its temperature, where blue is the coldest and red is the warmest (Rissler, 2023). Permission granted by the author; Christian Rissler*

In the master's thesis by Rissler (2023), an analysis of the design described above in the text and depicted in Figure 1 was conducted on the solar dryer onsite in Bhutan. The goal was to study the temperature change in each component of the solar dryer, such as the heat exchanger, absorber, heat storage, and the drying chamber at different air flows. The airflow used in the tests was 2 l/s, 4 l/s, 10 l/s, 14 l/s, and 18 l/s, and the food used in the experiments was ginger.

The conclusions from his experiments were that the heat exchanger's performance decreased when

the flow was increased; it was at its maximum efficiency when the flow was at 2 l/s and started to plateau between 14 l/s and 18 l/s, as can be seen in Figure 3. However, the heat flux between the heat exchanger's sides was more or less constant regardless of flow, but here 10 l/s gave the highest heat flux. According to Rissler (2023) this raises questions about whether the heat exchanger is worth the complexity and cost it adds to the construction of the dryer (Rissler, 2023).

Unlike the heat exchanger, the absorber had an increase in performance with higher flows but also started to plateau after 10 l/s. The temperature in the chamber reached a peak value of around 40 °C when the flow was set to 10 l/s or more, as can be seen in Figure 2. The drying rate, as shown in Figure 4, increased with increasing flow and showed no end to this trend. If high drying is the primary goal, maximizing the flow is the way to go for this interval. If high temperature is the goal, then a flow of 10 l/s is optimal (Rissler, 2023).

Regarding the heat storage, results show that 6 l/s and 10 l/s had the most heat retained at the end of the experiments. Rissler (2023) concludes that since the bottles take up space that could be used for food, and the dryer already functions as heat storage, it is uncertain whether the bottles are beneficial during this experiment (Rissler, 2023).

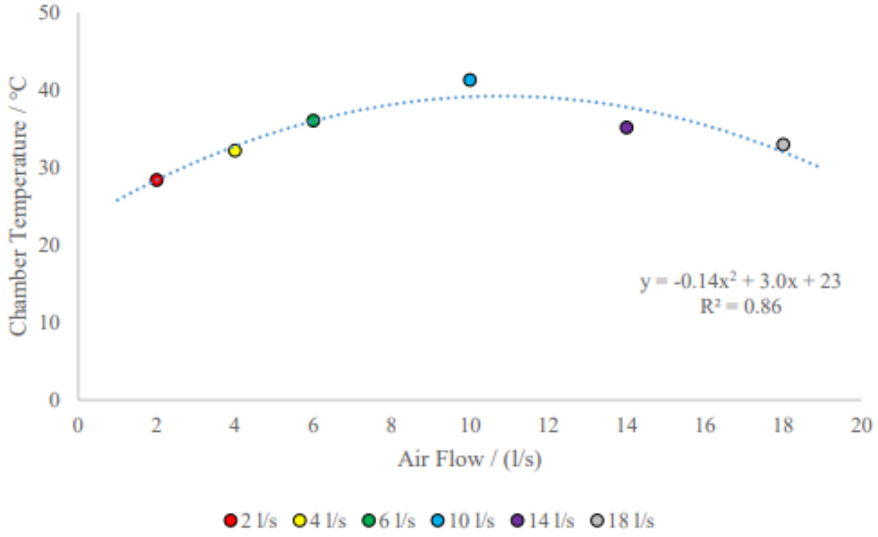

Figure 2: *The average chamber temperature plotted over flow. Each dot is the average of several experiments. The trendline is a dotted blue line and is based on the average values seen in the plot (Rissler, 2023). Permission granted by the author; Christian Rissler*

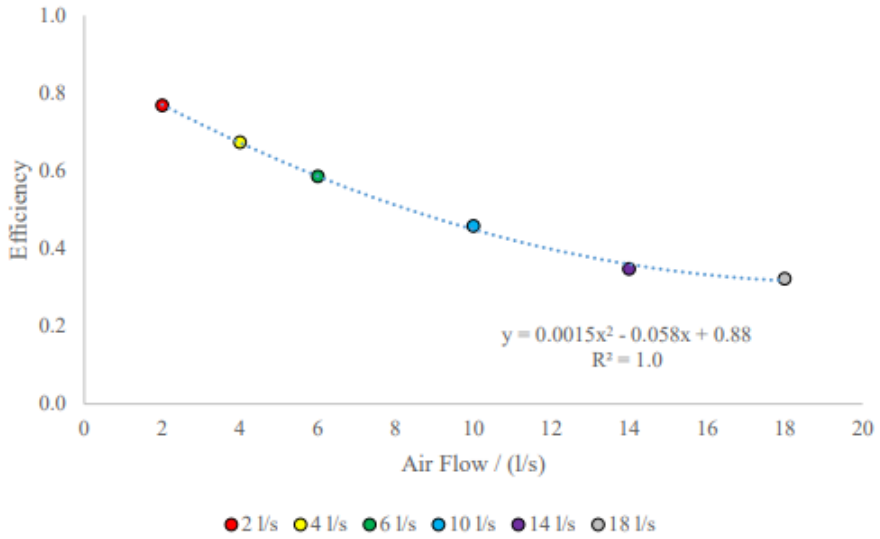

Figure 3: *The average efficiency of the heat exchanger plotted over flow. Each dot is the average of several experiments. The trendline is a dotted blue line and is of the second order and based on the average values seen in the plot (Rissler, 2023). Permission granted by the author; Christian Rissler.*

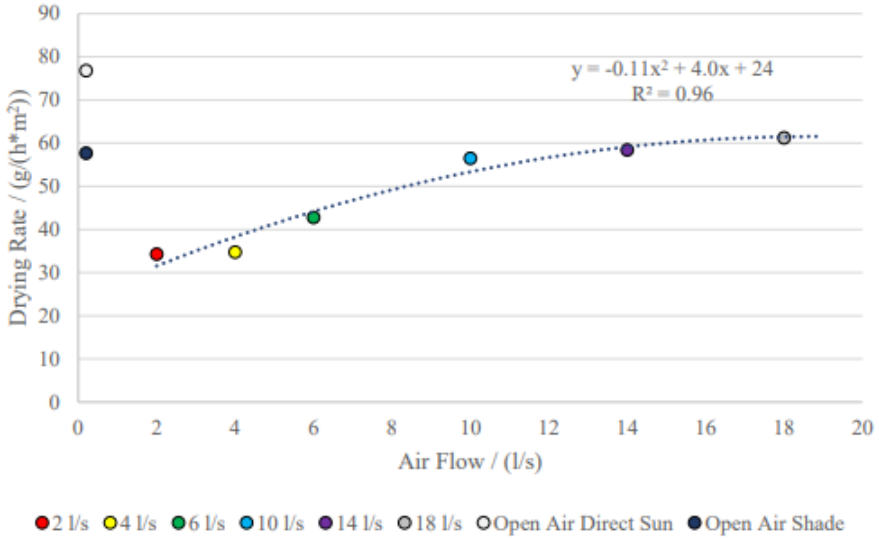

Figure 4: *The average drying rate plotted over flow. The trendline does not include the open-air drying experiments (Rissler, 2023). Permission granted by the author; Christian Rissler*

2.2.2 Second Design

The second design of the solar dryer to be simulated in this project has a slightly different design compared with the first one. The dryer still consists of a heat exchanger, absorber, heat storage, a drying chamber with five shelves, an internal fan, and an external fan. However, the new design features a larger absorber that extends from the bottom to the top of the dryer, and it has also a steeper angle of 45° compared to the previous 30°. Other design changes include mounting the inlet at the bottom of the dryer and placing the heat exchanger under the drying chamber. The outlet

is located at the back of the dryer. All of this is illustrated in Figure 5, and the airflow direction in the dryer is also depicted in Figure 5. This design was created by two students, Jamtsho and Om (2023).

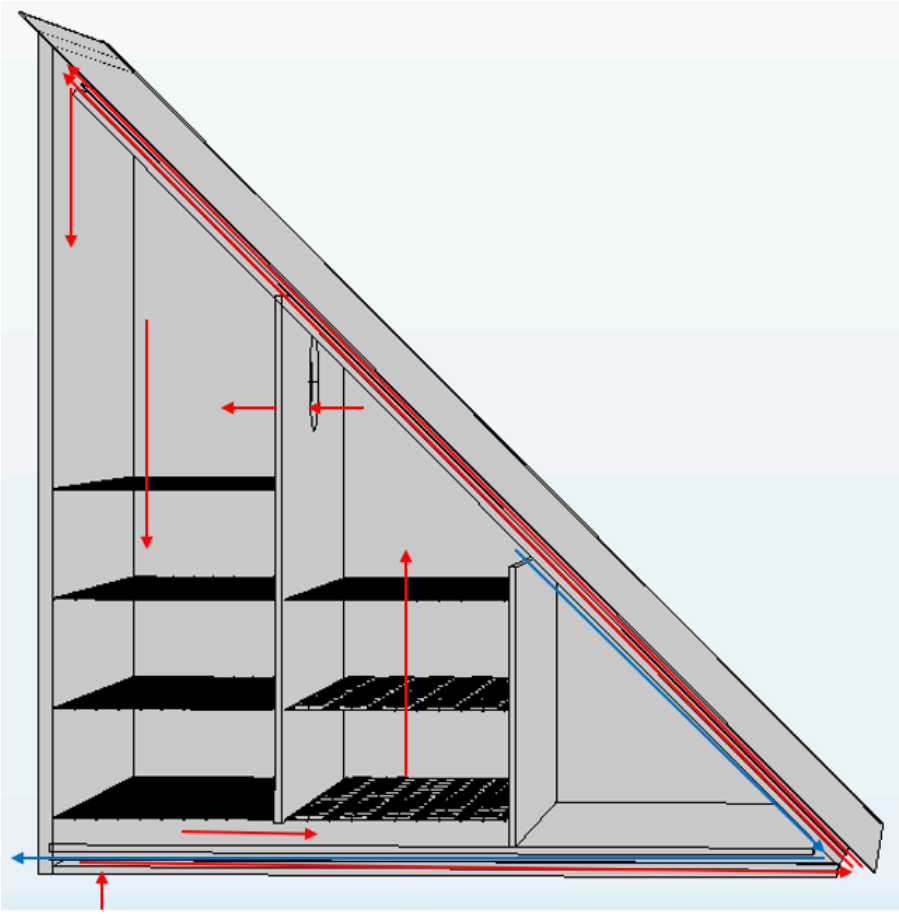

Figure 5: *The new dryer with the path of the airflow.*

Some goals of their study were to see how the number of trays influenced the drying rate, how the internal flow of air circulation within the dryer impacted its drying efficiency, and to what extent the size of the absorber contributed to increasing the efficiency of the dryer (Jamtsho & Om, 2023). They conducted their experiments in a controlled laboratory environment on campus at Lund University. They also did some testing with a larger internal fan that could run with a much higher flow without risking overclocking the fan.

The study showed that higher flow, particularly those generated by a powerful external fan, resulted in the most effective drying rates. Jamtsho and Om (2023) recommended using a fan with a higher voltage rating, which is likely to yield better drying results. Also, the size and placement of internal fans influences the drying rate inside the drying chamber. Futhermore, placing the fan in an optimal position and even increasing the number of internal fans could be something to test to enhance the drying process.

The number of drying trays within the drying chamber was found to impact the drying rate. A higher number of trays resulted in a decrease in the drying rate, while a lesser number of trays led to increased drying rates (Jamtsho & Om, 2023).

Their design showed similar behaviour for the absorber and the heat exchanger as in the first design. The absorber demonstrated its highest efficiency with the highest flow, while the heat exchanger achieved its highest efficiency with the lowest flow (Jamtsho & Om, 2023).

2.3 Airflow

Airflow is the movement of air, and air behaves like a fluid, meaning that the particles naturally flow from areas with higher pressure to areas with lower pressure. The measurement used for airflow is air per unit of time, which can be described as volumetric flow rate or mass flow rate. The airflow can be created by using mechanical devices such as electric or manual fans, but it can also be a function of different pressures in the environment. Since airflow has the same behaviour as a fluid, it also exhibits both laminar and turbulent flow patterns. With the help of the ideal gas law, air density can be described as a function of temperature and pressure (Briney, 2018). The ideal gas law (The Engineering ToolBox, 2003c):

$$pV = nRT \tag{1}$$

Where p is the pressure, V is the volume, T is the temperature, n is the amount of substance and R is the ideal gas constant, 8.314462618... $\mathrm{kgm^2s^2k^{-1}mol^{-1}}$.

2.3.1 Laminar flow

In fluid dynamics, laminar flow is characterized by the fluid's particles following smooth paths in parallel layers, moving along each other with little or no mixing. Laminar flow occurs at lower velocities, making the fluid flow without any mixing between the layers (Streeter, 1961). A flow remains laminar as long as the velocities are below the threshold for the flow to become turbulent. This is determined by the Reynolds number, which is a dimensionless parameter characterizing the flow. For a flow to be characterized as laminar, the Reynolds number needs to be below approximately 2 000 (Comsol, 2023). The Reynolds number is defined as (The Engineering ToolBox, 2003e).

$$Re = \frac{uL}{v} = \frac{puL}{\mu} \tag{2}$$

Where p is the density of fluid, u is the flow speed, L is the characteristic length, μ is the dynamic viscosity of the fluid and v is the kinematic viscosity of the fluid.

2.3.2 Turbulent flow

Turbulent flow is when flow experiences changes both in pressure and velocity, like swirls or mixing. In turbulent flow the speed of the fluid is constantly undergoing changes in both magnitude and direction (Britannica, 2023). Turbulent flow can be observed in most fluid flows in nature, like rivers or weather storms. But turbulent flow can also be created in engineering application, such as in the aerodynamics of all vehicles such as cars, planes and ships (Simscale, 2023c). Turbulent flow is caused by excessive kinetic energy in fluid flows that overcomes the damping effect of the fluid's viscosity (Britannica, 2023). As previously mentioned in the paragraph about laminar flow, the Reynolds number defines when a flow is a turbulent or laminar flow. If the Reynolds number is above 2 000 the flow is turbulent. Figure 6 shows the behavior of both laminar flow and turbulent flow in closed pipe.

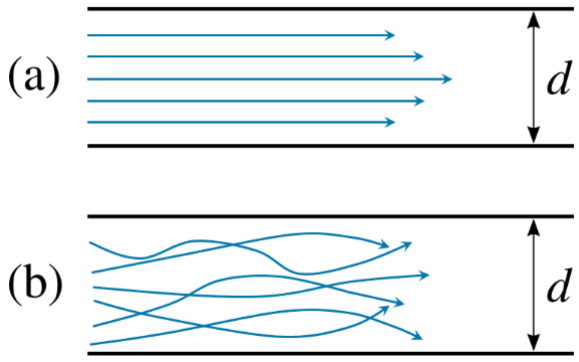

Figure 6: *(a) Laminar flow in a closed pipe, (b) Turbulent flow in a closed pipe. The laminar region is smooth with less chaos because the turbulent flow has high momentum convection (Simscale, 2023b). Permission granted by: Simscale*

2.4 Heat transfer

Heat transfer can be considered as a mechanism that transports energy from one physical object to another, and there are three main methods describing this phenomenon: radiation, convection, and conduction. The three methods are shown in Figure 7.

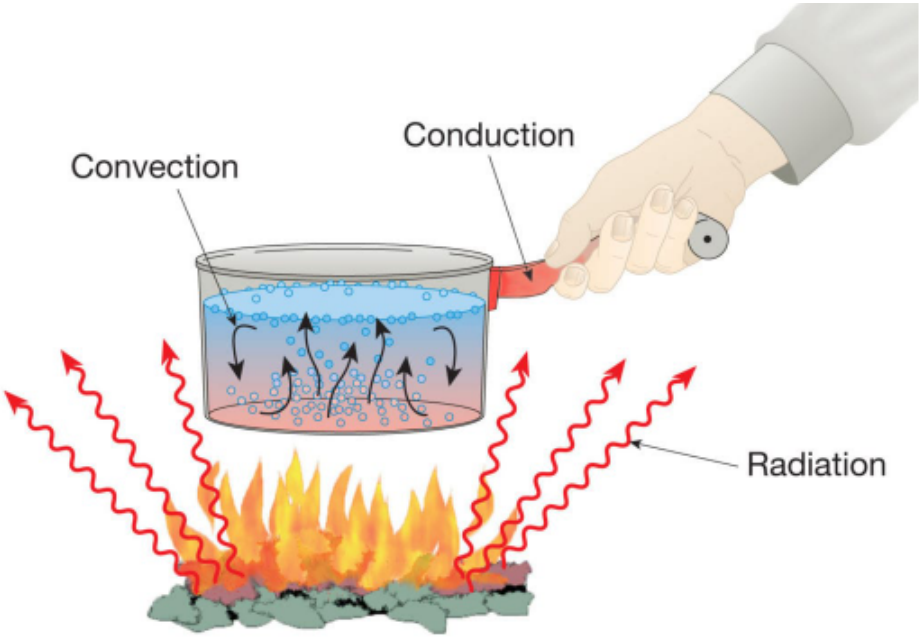

Figure 7: *Radiation, convection, and conduction (Simscale, 2023a). Permission granted by: Simscale*

2.4.1 Radiation

Radiation in heat transfer is the emission or transmission of energy in both directions between two bodies of mass. The energy emits or transmits more from the body with the higher temperature to the body with a lower temperature. However, energy also emits or transmits from the body with the lower temperature to the body with higher temperature. This emission or transmission is in the form of electromagnetic waves, and the wavelength of the electromagnetic waves is mainly in the infrared range, but it depends on the source of the emission or transmission. The waves in

radiation or thermal radiation do not need a material medium to transfer the energy (Ganji & el al., 2017). For instance, thermal radiation from a solid body/surface, the medium the radiation passes through could be a vacuum, gas, or liquid. The medium's atoms and molecules can absorb, reflect, or transmit the radiation energy. Radiation is most efficient if the medium is a vacuum, since there are no atoms or molecules and therefore the radiation energy is not decreased, and fully transmitted. When it comes to gas, for example the medium is air, the air molecules can absorb or reflect the energy, leading to energy losses. A surface that absorbs all incoming radiation and reflects none is called a black surface or a black body; a black body is a perfect radiator (Ganji & el al., 2017). The equation for the rate at which energy is radiated from a body is given by (The Engineering ToolBox, 2003d):

$$q = \sigma \epsilon A T^4 \tag{3}$$

Where q is the rate of energy emission from the surface, A is the surface area of the radiator, ϵ is the emissivity(ratio of the emission from a real "gray" surface to the emission from a perfect "black" surface) of the surfaces and σ is the Setfan–Boltzmann constant, $5.67{\cdot}10^{-8}\mathrm{W}/(\mathrm{m}^2\mathrm{K}^4)$.

2.4.2 Convection

Convective heat transfer occurs when heat is transmitted between two bodies by a current of moving gas or fluid. In free convection, air or water moves away from the heated body as the air or water warms up, pushing the cooler air or water down, creating a kind of circulation, as seen in Figure 7. In forced convection, air or water is moved by force across the body surface (such as in wind, a fan, a pump, or water currents) and efficiently removes heat from the body (Sokolova, 2019). Convection is a very efficient way for heat to transfer because it maintains a steep temperature gradient between the body and surrounding fluid (Sokolova, 2019). The equation for convection can be expressed as (The Engineering ToolBox, 2003b):

$$q = h_c A \Delta T \tag{4}$$

Where A is the surface area, h_c is the convective heat transfer coefficient of the process and ΔT is the temperature difference between the surface in contact with the fluid and the average temperature of the fluid.

2.4.3 Conduction

Conduction is the transfer of thermal energy through matter, i.e., solids, liquids, or gases. In other words, conduction is the transfer of energy from the more energetic to less energetic particles of a substance due to interaction between the particles (Shahidian & el al., 2020). This means that different materials have different conductivities, giving some materials the ability to transfer heat better than other materials. The equation for conductive heat transfer is given by (The Engineering ToolBox, 2003a).

$$q = (\frac{k}{s}) A \Delta T \tag{5}$$

Where A is the surface area, k is the thermal conductivity of material(W/mK or W/m°C), s is the material thickness and ΔT is the temperature gradient difference over the material.

3 Method

The methodology for this master's thesis involved computer simulations using the software COMSOL Multiphysics to analyze the results from the simulations and make adjustments based on the results. The workflow for COMSOL is shown in Figure 8.

3.1 COMSOL Multiphysics

COMSOL Multiphysics is a mathematical modelling software used in various fields including engineering, scientific research, and manufacturing. It was founded by Svante Littmarck and Farhad Saeidi in 1986 in Stockholm, Sweden. Since then, the company has grown into a group of subsidiaries spread around the world (Comsol, 2023a).

The software is a simulation platform capable of both multiphysics and single-physics modelling. COMSOL comes with a model builder that provides a simulation environment and a consistent modelling workflow throughout the process. The initial step is to construct the model using three-dimensional geometric bodies, such as cylinders and blocks. The next step is to import the correct materials and define them in the appropriate areas. Subsequent steps include physics-based modelling, equation-based modelling, meshing, studies and optimization, solvers, and finishing with visualization and results evaluation (Comsol, 2023c).

3.2 COMSOL

The first step was to become familiar with COMSOL and understand the workflow in the software. This was achieved by watching tutorial videos provided by COMSOL on their website, covering the basics of the program. However, it became evident that these tutorials were insufficient to gain the necessary knowledge and understanding of the software to set up simulations for the solar dryer. Upon receiving advice from the supervisor, it was recommended to explore COMSOL's documentation and introduction guides, which offer step-by-step instructions on setting up different models and simulations.

One of these introduction guides was for the CFD module, where CFD stands for computational fluid dynamics. The CFD module includes modelling stationary and time-dependent fluid flow problems in two- and three-dimensional spaces, providing insight into fluid flow interfaces and how to set up and solve various problems related to fluid flows (Comsol, 2022a). After completing the CFD module, an instruction guide for the heat transfer module was followed to gain a good understanding of setting up heat transfer simulations, including conduction, convection, and radiation, and studying the influence of heating and cooling in devices and processes (Comsol, 2022b). After completing several instruction guides, work began on setting up the solar dryer simulations.

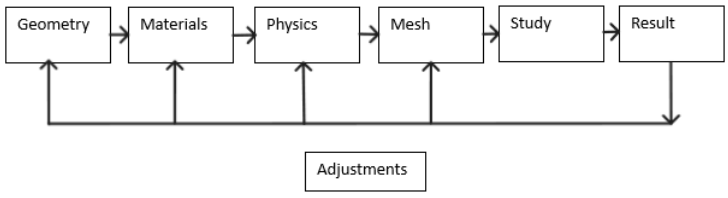

Figure 8: *The work process in COMSOL.*

3.3 Building Designs in COMSOL

The process began by setting up COMSOL, selecting a new model wizard project, and choosing the spatial dimension for the project. For both designs, 3D dimensions were selected. Next, there was the option to add physics to the project and choose between different studies, stationary or time-dependent. The decision was made not to add any physics or studies at this stage, in order to focus on the geometric shape of the dryer and ensure it was set up correctly before introducing additional complexities.

3.3.1 Geometry

The measurements for the first design were taken from Figure 9, and the layout was based on Figure 1. For the second design, measurements were taken from the built prototype in person.

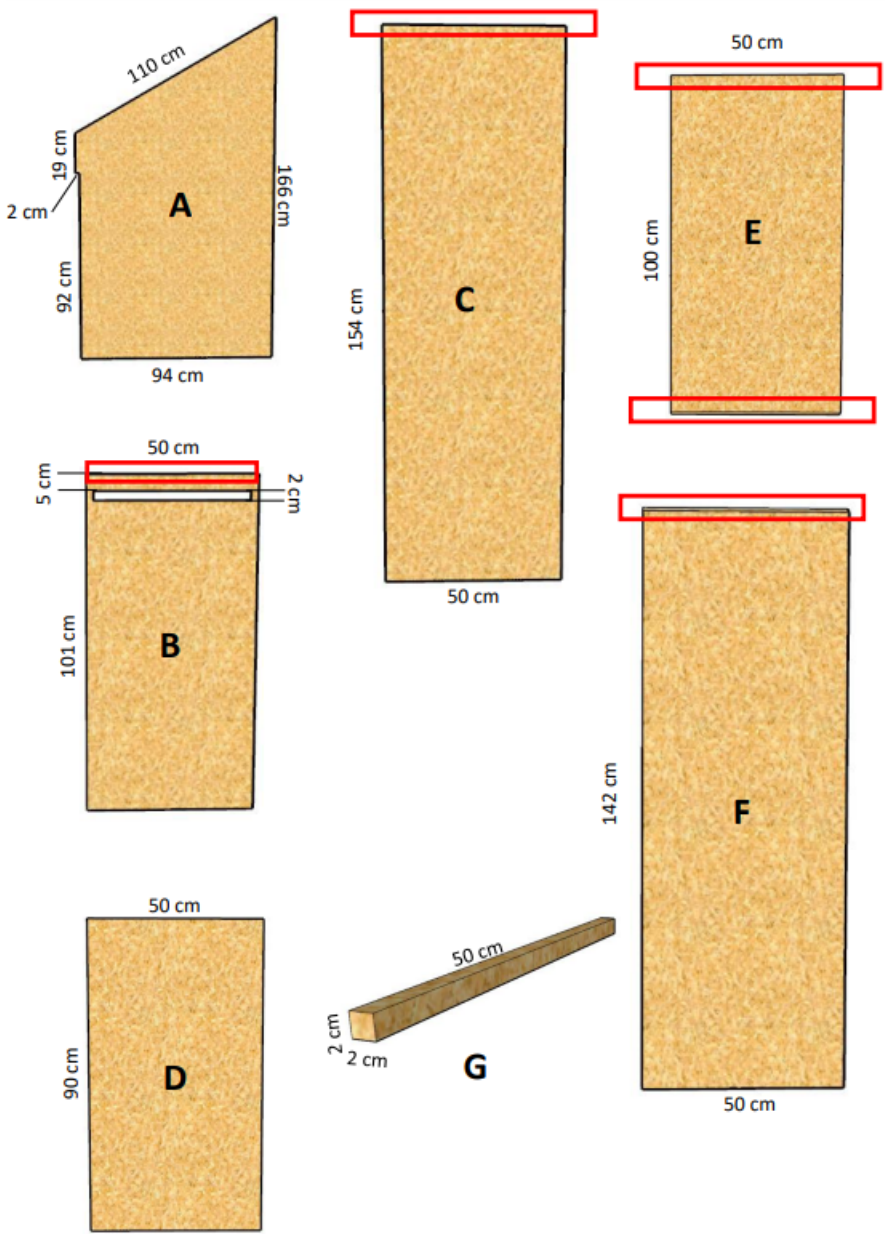

Figure 9: *The food dryer´s different parts and the measurements for the parts (Probert, 2022). Permission granted by the author: Adam Probert*

Doing the geometry part for the two designs the following steps were used:

1. The inner shell or the air volume began with a block that had the measurements for the inner area of the design. To determine the correct angle for the top of the dryer, another block was added at the desired angle, and a boolean operation called difference was used to subtract the two blocks from each other. The result is shown in Figure 10.
2. The outer shell, in the form of the walls of the dryer, was created in the same way as the inner shell, but with a larger block to achieve the correct thickness of the walls.

3. The next step in the process was to fill the inner shell with blocks to create the drying chamber, the absorber, and the heat exchanger. The interior fan was created using a cylinder, and a block was added for the glass on top of both the inner and outer shells.

4. The shelves were created for the two drying chambers by forming a grid of cylinders. This process involved six steps for each chamber. Firstly, a cylinder was selected, and its radius was set to 0.5 mm. The length of the cylinder depended on whether it was oriented in the x or y-direction, matching either the length or the depth of the chamber. The cylinders were positioned 5 mm away from the walls. In the second step, an array was utilized to generate x number of cylinders, evenly spaced from each other. The third step mirrored the first, adjusting the cylinder length based on the orientation chosen previously. Step four replicated the second step. Following step four, a shelf was formed, as depicted in Figure 11. Step five involved utilizing a boolean operation called union, which combined the two arrays. Finally, step six entailed creating the desired number of shelves, each spaced 15 cm apart from one another, achieved through an array operation on the union created in step five.

After the steps described above the geometry phase of the project was done, the geometric shapes of the two designs can be seen below in Figure 12 and Figure 13.

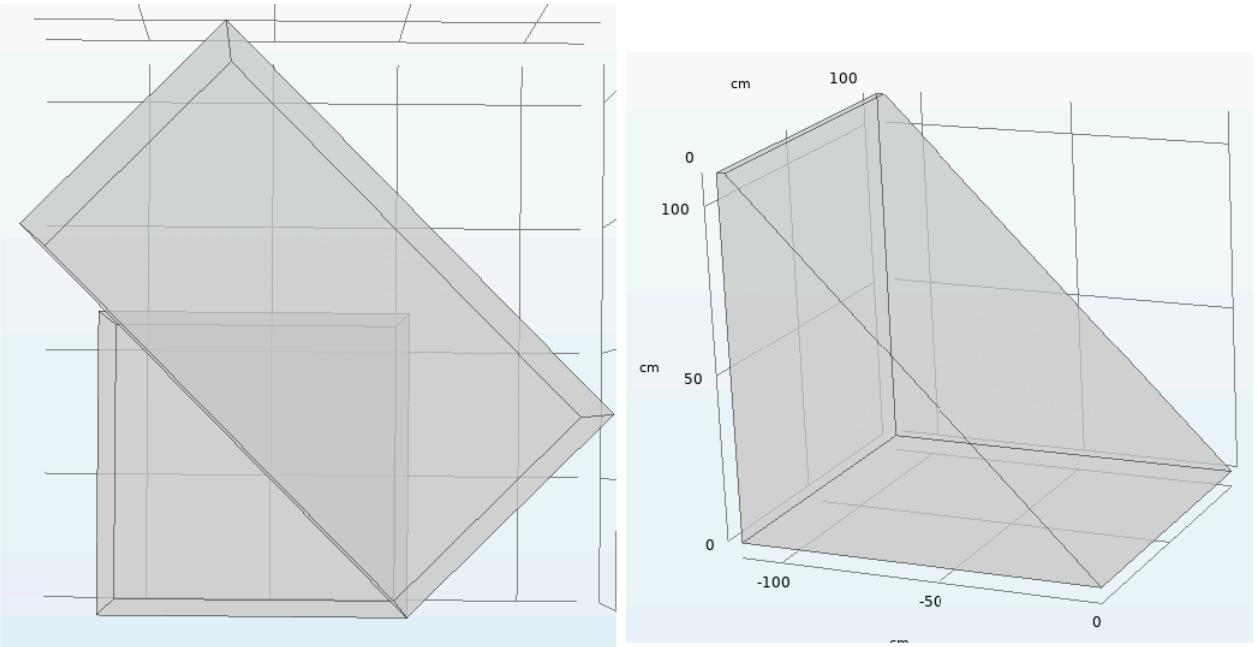

Figure 10: *The inner shell of design two of the solar dryer. To left picture shows before the boolean operation difference has been used. The right picture after the difference have been used.*

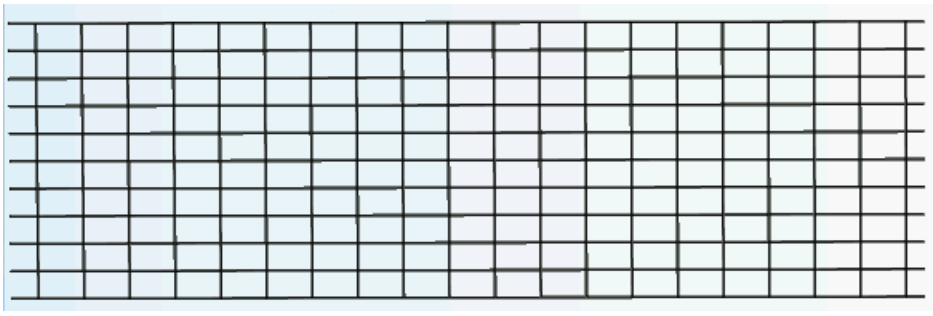

Figure 11: *The grid of one shelf, with rectangular holes that is 15 cm*^{2}.

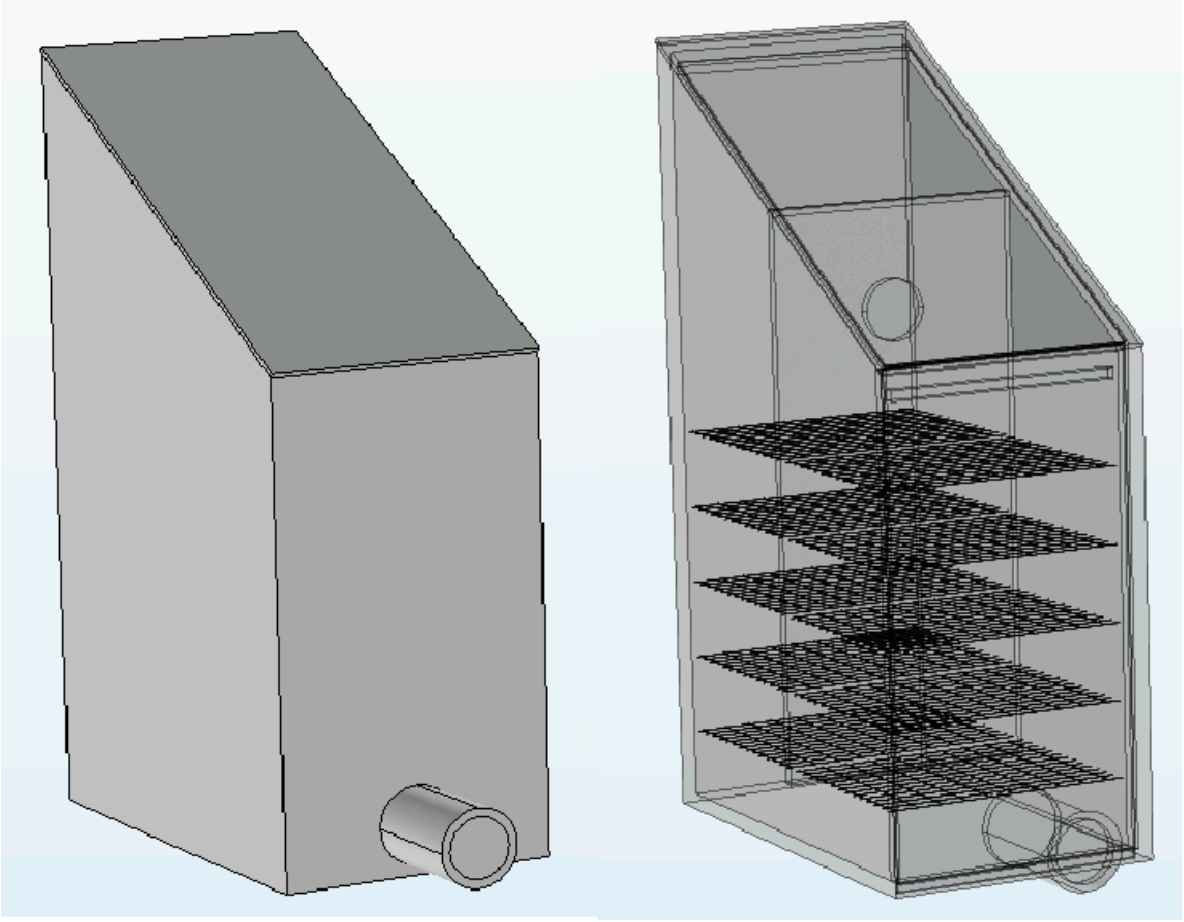

Figure 12: *The first design with 10 shelves, to the left without transparency and to the right with transparency.*

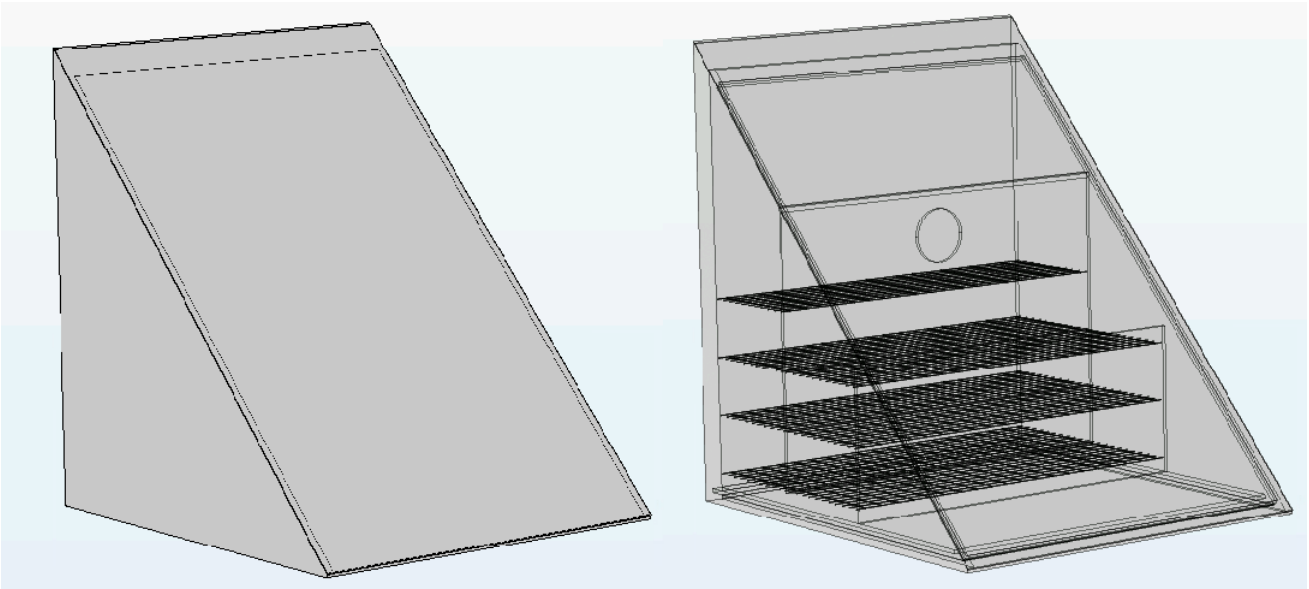

Figure 13: *The second design with 7 shelves, to the left without transparency and to the right with transparency*

3.3.2 Material

After the geometry step, the next step is to select the materials for the different domains of the dryer. COMSOL has a material library, which is a database with materials that already have all the different material properties. The materials selected for the different domains were: aluminum for the absorber and heat exchanger, steel for the shelves, wood (pine) for the walls, air for the air volume, and silica glass for the glass that lays on the top of the dryer. Plywood was not in the material library, so the decision was made to use pine wood instead. This decision was based on the fact that the project's main focus was not on heat transfer but on airflow and pressure, so the material of the walls has very little effect on the airflow.

3.3.3 Physics

The step after adding the materials was to add the physics. Laminar flow was the first physics to be added, chosen because the speed of the fan is low and constant, ensuring the Reynolds number will not exceed the limit for turbulent flow. Here, the inlet and outlet were added, with the inlet flow set to 10 l/s and the outlet pressure set to zero Pa.

The next physics added was heat transfer in solids and fluids. Adding this also included the multiphysics interface, nonisothermal flow. This interface couples the two interfaces, laminar flow and heat transfer in solids and fluids. The next task was to define the walls domain as solids and the air domain as fluid. In addition, the boundaries inflow and outflow were added and set to the same surface as the inlet and outlet in laminar flow. The inflow temperature was set to 25°C. Also, the boundaries' heat flux was added, both for the walls to simulate heat losses by setting a negative value, and for the heat exchanger and absorber to a fixed heat rate to simulate some heat exchange from the surfaces to the air domain.

3.3.4 Mesh

After creating the geometry and assigning the physics to the model, the next step was to build the mesh. The mesh used for a model geometry plays an instrumental role in how the model is solved, as it determines factors such as(Comsol, 2023b):

- How the geometry is divided
- With what shape or element type the geometry is divided
- The size, density, and number of elements in the geometry
- The element quality

The meshing process was streamlined by using automatic meshing of the model geometry. This was accomplished by selecting physics-controlled mesh and starting with the largest element size, which was set to extremely coarse. The intention was to progressively reduce the element size of the mesh during the course of the project to achieve a more accurate simulation. However, this was not implemented due to time constraints. The different element sizes can be observed in Figure 14.

3.3.5 Study

The last step in COMSOL was to add a study to the model, this step is necessary to be able to compute the model. For both designs, a stationary study was chosen, since all the field variables do not change over time.

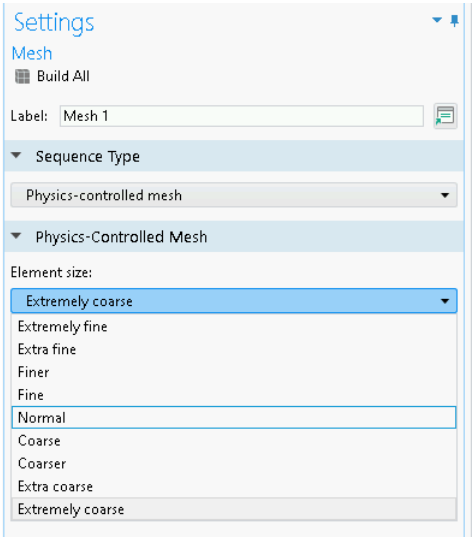

Figure 14: *The different element size in a physics-controlled mesh*

4 Results

4.1 Airflow for First Design

4.1.1 Empty dryer with 10 shelves

The airflow inside the dryer is moving in the direction as designed with an average speed of 0.19 m/s inside the air volume. The average speed was calculated by using derived average values in COMSOL, which were used for all the simulations. In the area marked with 1 in Figure 15, the internal fan is pushing air towards the back wall, and the air is distributed both in an upward and downward direction with the internal fan speed was set to 10 l/s. This creates what can be observed in the area marked with 2 in Figure 16; a vortex of air in the upper left chamber at the intake of the drying chamber. In the second drying chamber, there is a similar phenomenon occurring in the area marked with 3; halfway up the chamber, some of the air seems to get pushed back down, creating a larger vortex than the one in chamber one.

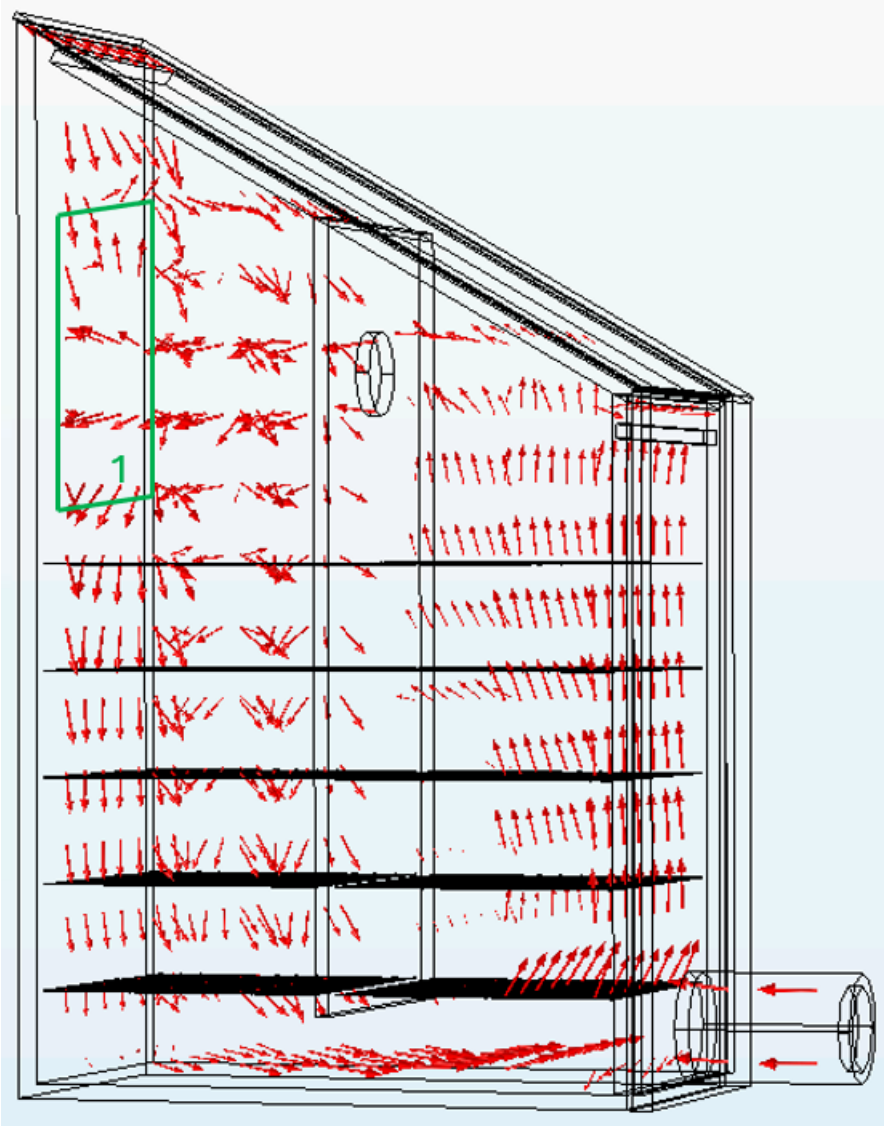

Figure 15: *Direction of the airflow inside the drying chamber. Internal fan and inlet fan size 120 mm, with a speed of 10 l/s. The distance between the shelves is 15 cm. The area marked with 1 shows the air is distributed both in an upward and downward direction when hitting the wall.*

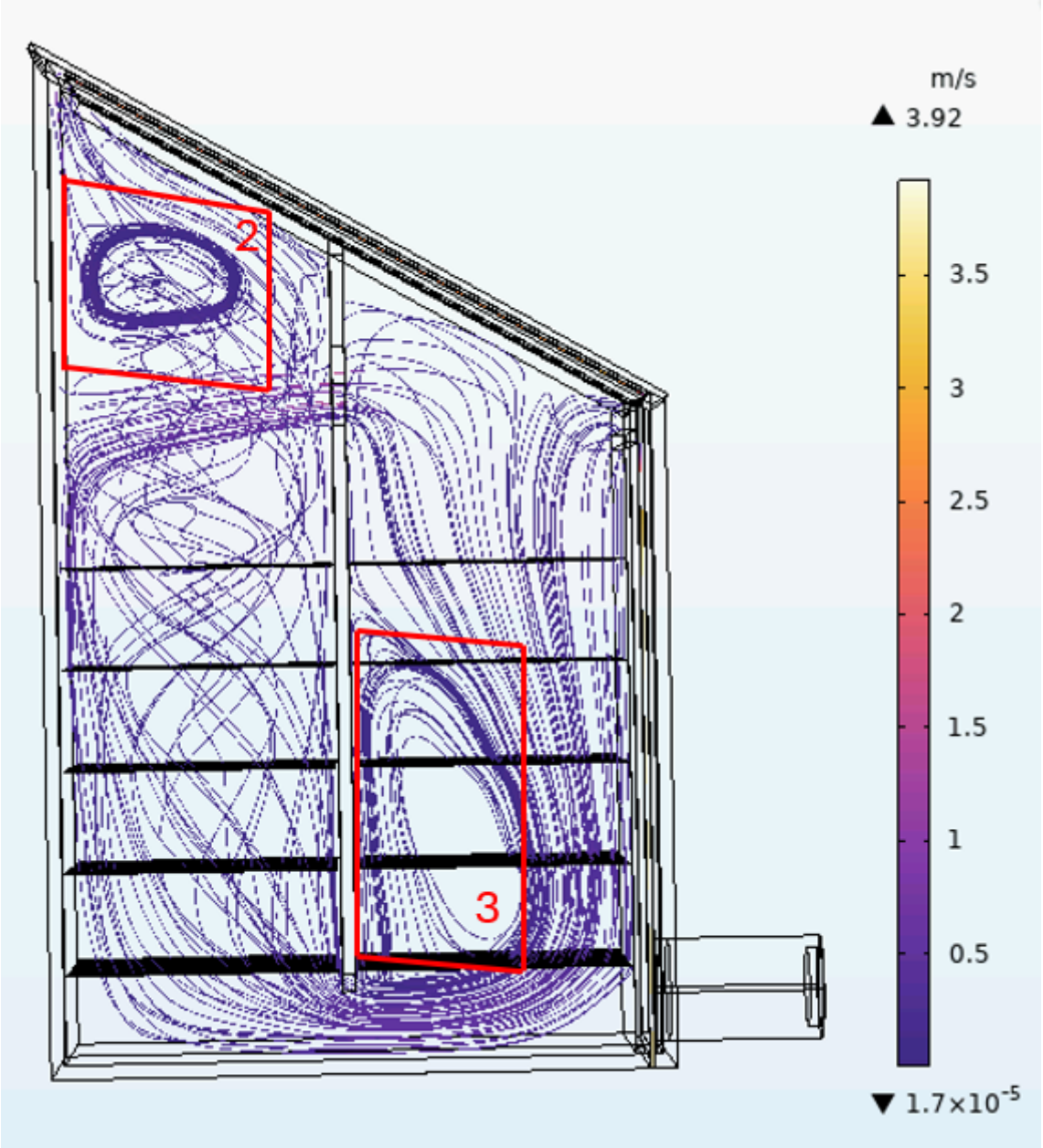

Figure 16: *The streamline of the airflow inside the air domain. The area marked with 2 shows the air vortex in chamber one and the area marked with 3 shows the air vortex in the second drying chamber.*

4.1.2 Dryer with 10 shelves, 2 shelves with slices of apples on them

Cylinders with a radius of 2 cm were added to the two bottom shelves in the second drying chamber to represent slices of apples. The apples were only added on two of the shelves because the simulation would not run when having apples on all the shelves, and due to lack of time, this problem was not solved.

The slices of apples appear to have a dispersion effect on the air, making the air vortex in the second drying chamber smaller in size. This can be observed when comparing the area marked with 2 in Figure 17 with the area marked with 3 in Figure 16. The air vortex in the first drying chamber has changed a bit, as can be seen in Figure 17 in the area marked with 1. The average speed inside the air volume was approximately 0.19 m/s, and the maximum air velocity decreased by two tenths, which is reasonable since the surfaces of apples are slowing some of the air.

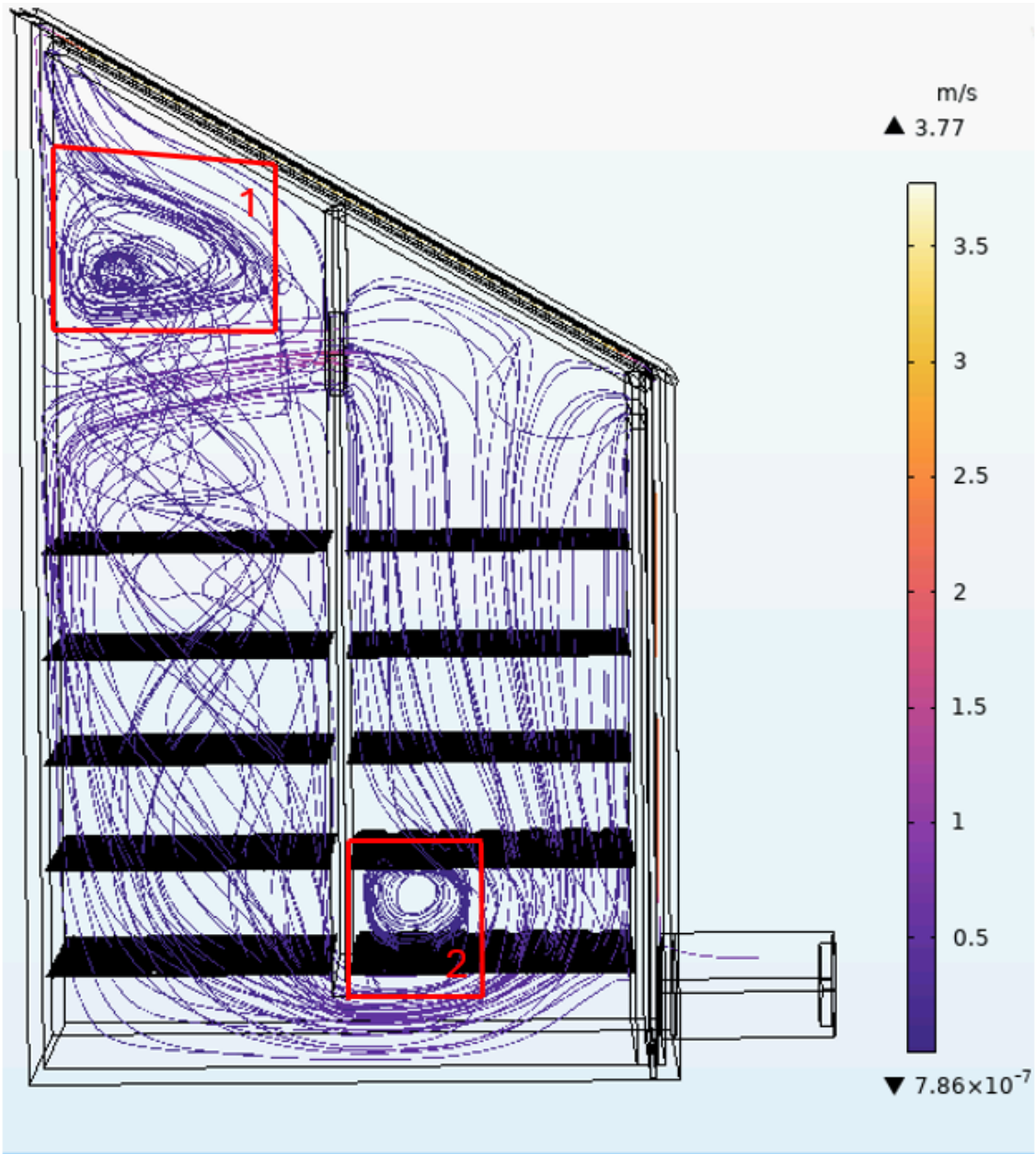

Figure 17: *The streamline of the airflow inside the air domain. The area marked with 1 shows the air vortex in chamber one and the area marked with 2 shows the air vortex in the second drying chamber.*

4.1.3 First design with design changes

Since there is a problem of the air vortex forming in the first drying chamber, the first simulation was to try to solve this by changing the size of the entry gap to the drying chamber by increasing it from 2 cm to 6 cm.

The result from this simulation was that the air entering the drying chamber seemed to move more towards the internal fan, as can be seen in the area marked with 3 in Figure 18. When comparing the area marked with 1 in Figure 18 with the area marked with 1 in Figure 17, it seems that the vortex in the first drying chamber has decreased. This could be an effect of what has been mentioned before, with air moving more towards the internal fan and less air feeding the vortex. This shows that this design change is in the right direction to remove the vortex in the first drying chamber.

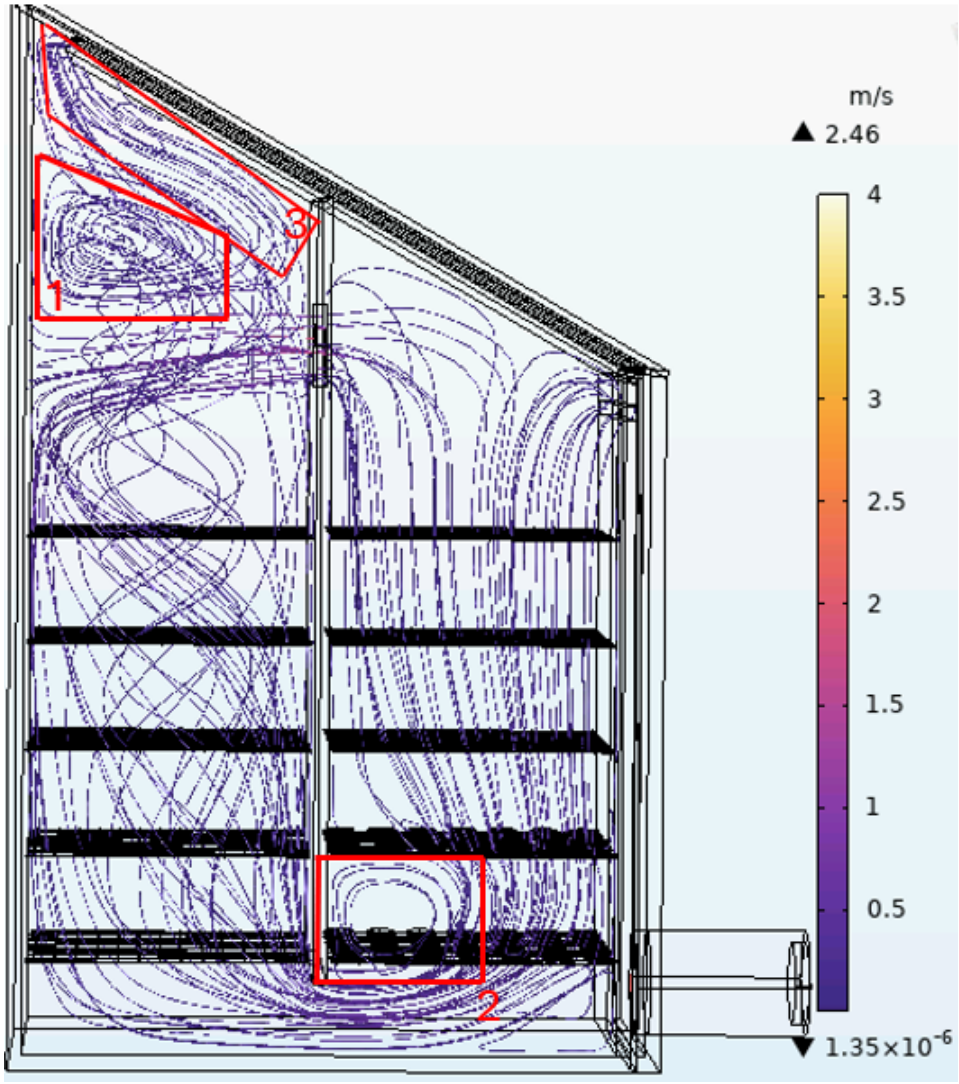

Figure 18: *The streamline of the airflow inside the air domain, with a larger entry gap to the drying chamber. The circles inside the marked areas is the cut points that was used to evaluated the speed inside the two vortex. The area marked with 1 shows the air vortex in chamber one and the area marked with 2 shows the air vortex in the second drying chamber. The area marked with 3 shows the air entering the drying chamber moving towards the internal fan.*

In simulation two, the parameter that was changed was the placement of the internal fan. The fan was placed 2 cm from the top edge of the middle panel. The result from making these two changes in the design had a positive effect on the vortex problem in the first drying chamber. As can be seen in the area marked with 1 in Figure 19, the vortex in the first chamber is more or less gone. When comparing the area marked with 2 in Figure 19 to the area marked with 2 in Figure 18, moving the fan has affected the vortex in the second drying chamber. This is a bit strange and hard to understand why, and to confirm that this actually happens, experiments would need to be carried out on the solar dryer. But it is outside the scope of this project.

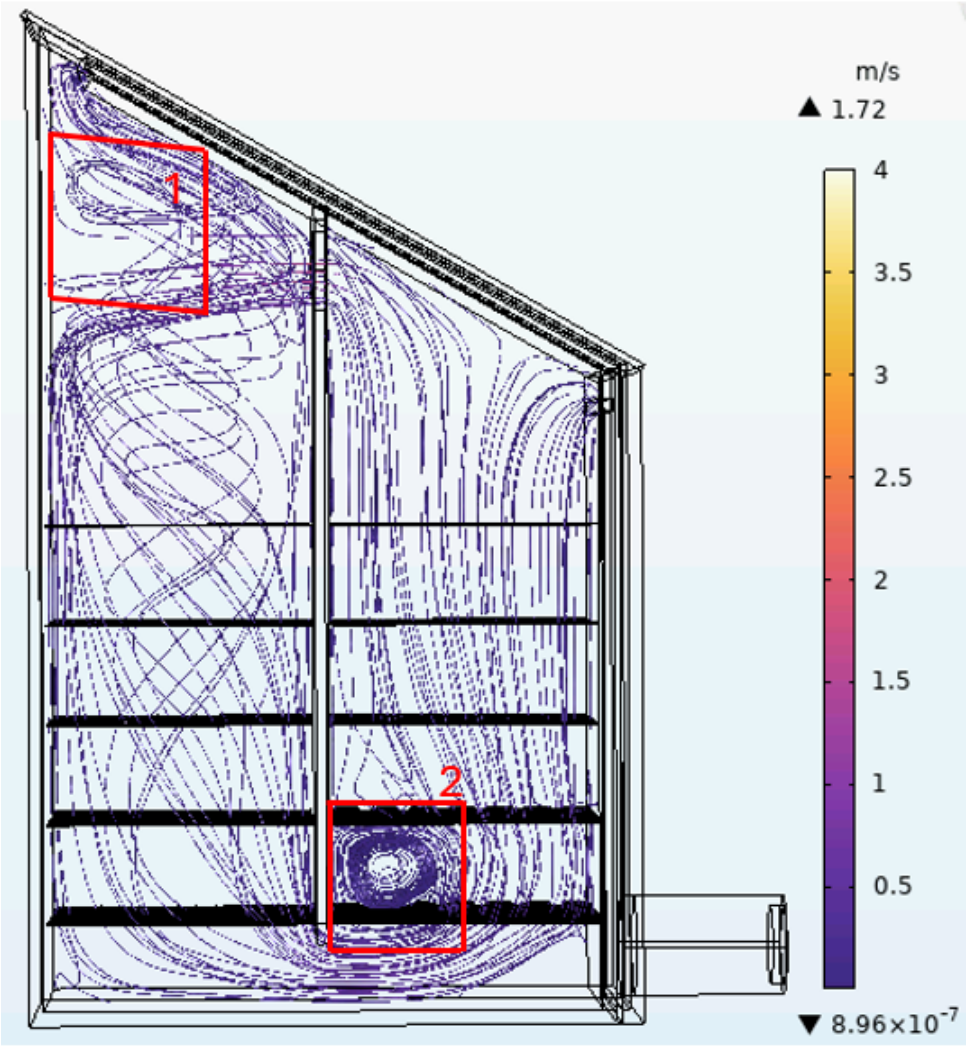

Figure 19: *The streamline of the airflow inside the air domain with a larger entry gap to the drying chamber and the internal fan is placed higher up. The area marked with 1 shows the air vortex in chamber one and the area marked with 2 shows the air vortex in the second drying chamber.*

For simulation three, two parameters were changed: the size of the internal fan and the inlet fan was increased to 140 mm, and the speed of the internal fan was set to 14 l/s. The vortex in the first chamber is still gone, as can be seen in the area marked with 1 in Figure 20. However, the vortex in the second chamber is still present, as can be seen in the area marked with 2 in Figure 20. The average speed inside the air volume was 0.21 m/s, with a maximum velocity of 4.17 m/s.

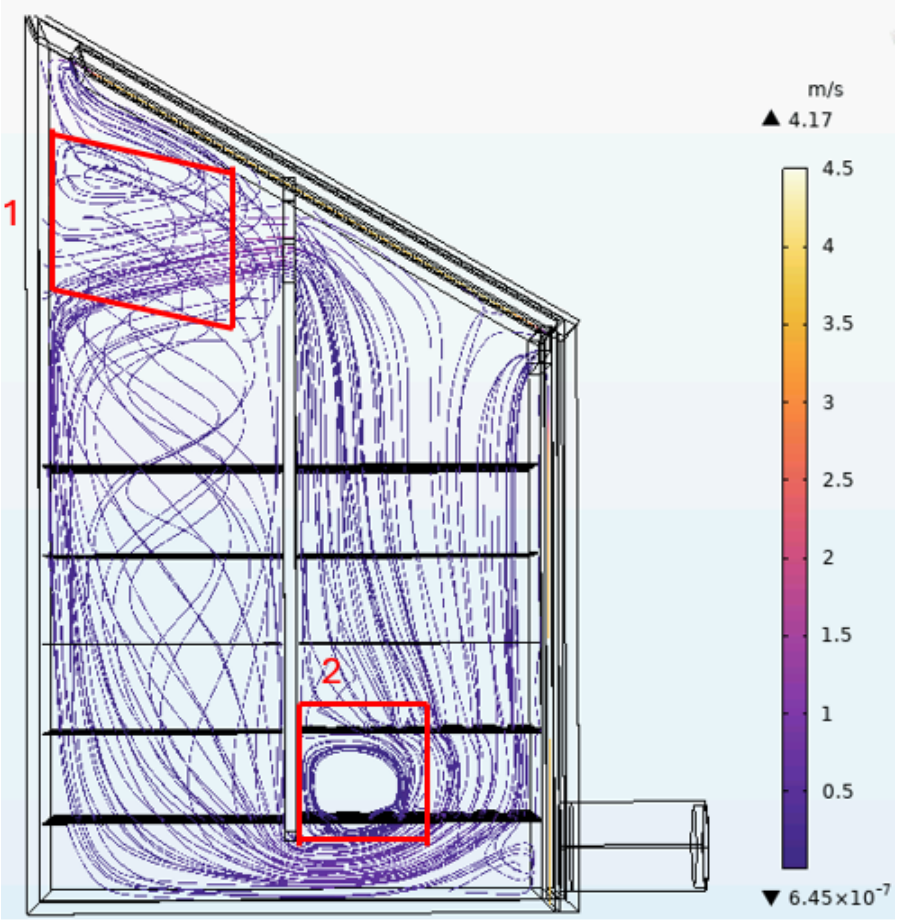

Figure 20: *The streamline of the airflow inside the air domain, with larger entry gap to the drying chamber and the internal fan is placed higher up. The size of the fans is 140 mm and the speed on the internal fan is set to 14 l/s. The area marked with 1 shows the air vortex in chamber one and the area marked with 2 shows the air vortex in the second drying chamber.*

4.2 Pressure First Design

4.2.1 Empty dryer with 10 shelves and 2 shelves with slices of apples on them

Comparing the pressure for the empty dryer with 10 shelves to the pressure when having two shelves with apples shows that there is almost no difference in pressure, as can be seen in Figure 21. The largest pressure drop for both simulations occurs when the air is reaching the absorber at the top of the dryer, decreasing from around 80 Pa to 60 Pa, as shown inside the green rectangles in Figure 21. The average pressure in the air domain for both simulations is 21.5 Pa, indicating that adding the apples has almost no effect on the pressure inside the air domain.

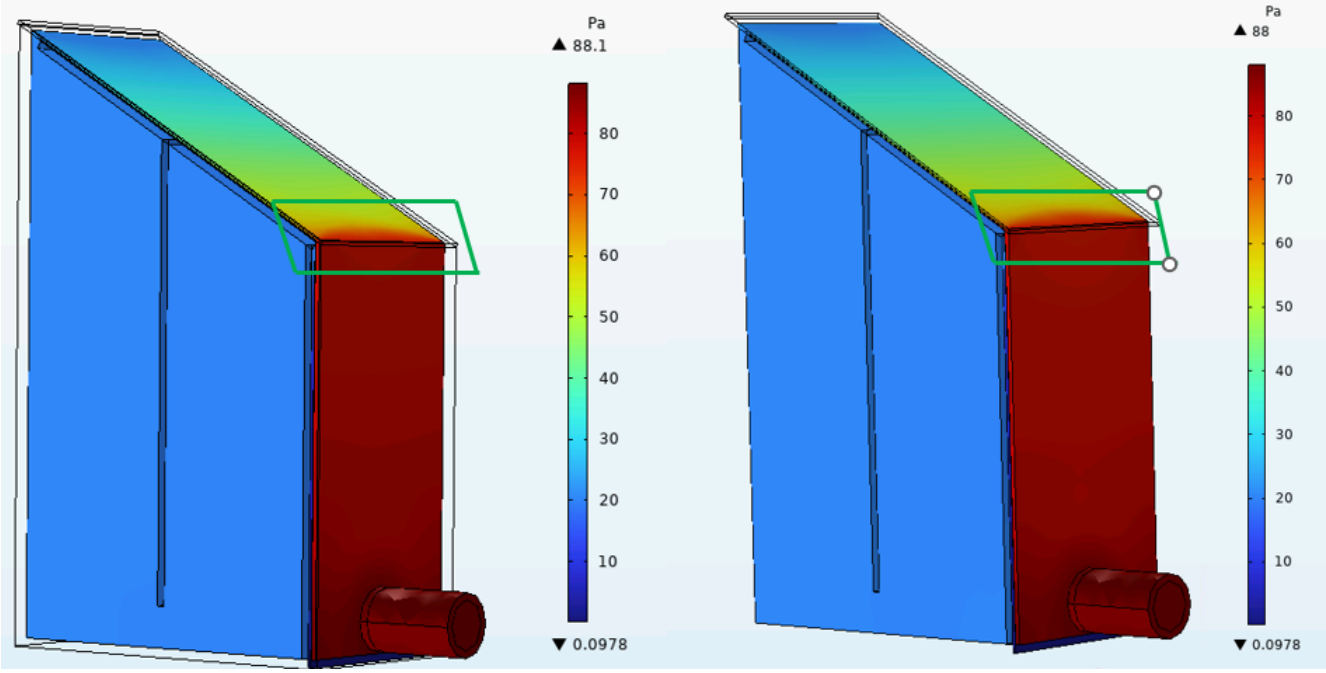

Figure 21: *The pressure in the air volume, to the left empty dryer with 10 shelves and to the right is 2 shelves with slices of apples on them. The area inside the green rectangle shows the largest pressure drop point.*

4.2.2 First design with design changes

The parameters that were changed do not seem to have a major effect on the pressure. The pressure inside the air volume still decreases substantially when the air reaches the absorber at the top of the dryer, as can be seen inside the marked area in Figure 22. The average pressure inside the air volume is 21.5 Pa, and it remained the same for all the simulations.

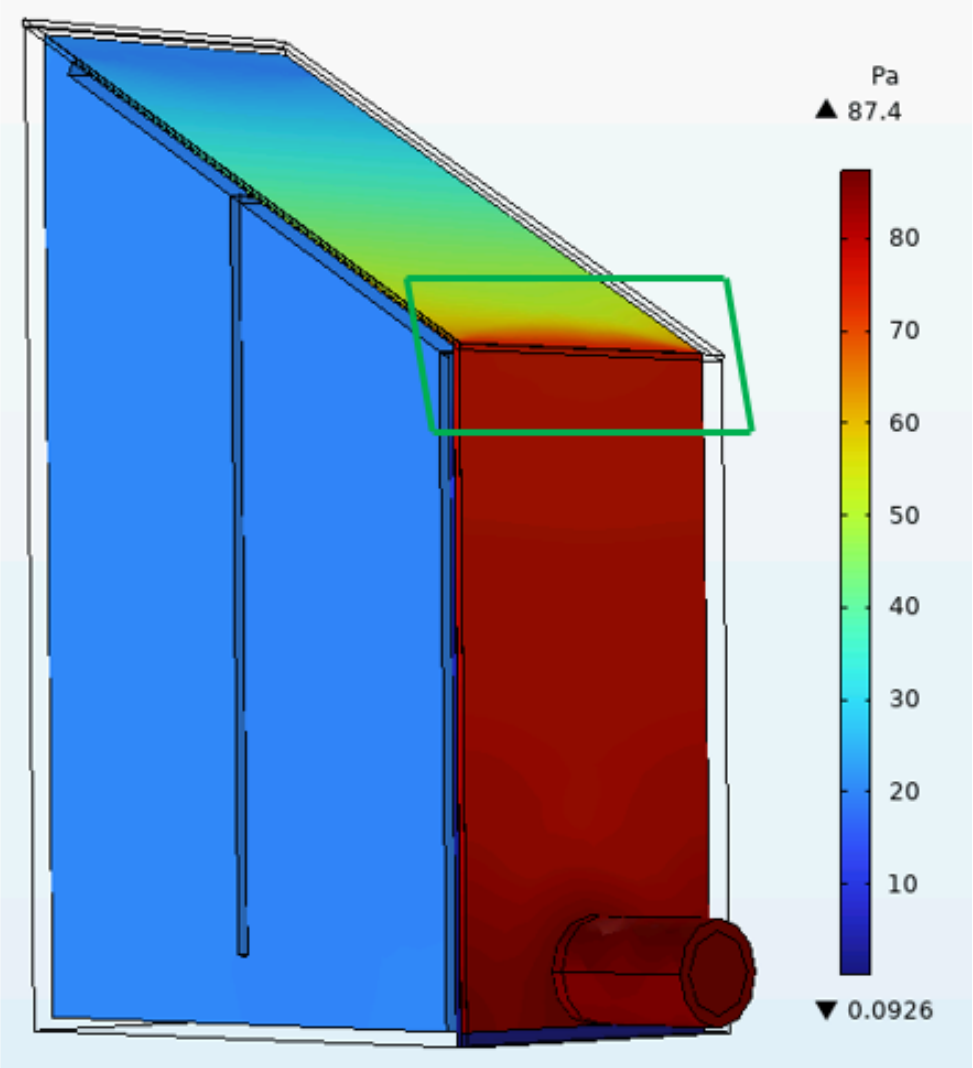

Figure 22: *The pressure inside the air volume, with a larger entry gap to the drying chamber. The mark area shows the largest pressure drop inside the air domain.*

4.3 Second Design

4.3.1 Empty dryer with 7 shelves

The airflow in this design is similar to the first design; both in the first drying chamber and in the second drying chamber, a vortex occurs. In the first drying chamber, the vortex is located in the upper part of the chamber, and in the second chamber, the vortex extends from above the third shelf to the bottom shelf. Some of the air also creates a vortex after it flows out of the second drying chamber towards the outlet. This can be seen inside the area marked with 1 in Figure 23. The average speed in the air volume is 0.16 m/s, and the air picks up speed when entering the second chamber, as can be seen in the area marked with 1 in Figure 24. The reason behind this is that the volume gets smaller, and since the same amount of fluid is flowing through a narrower region, the fluid must move faster to move the same volume of air.

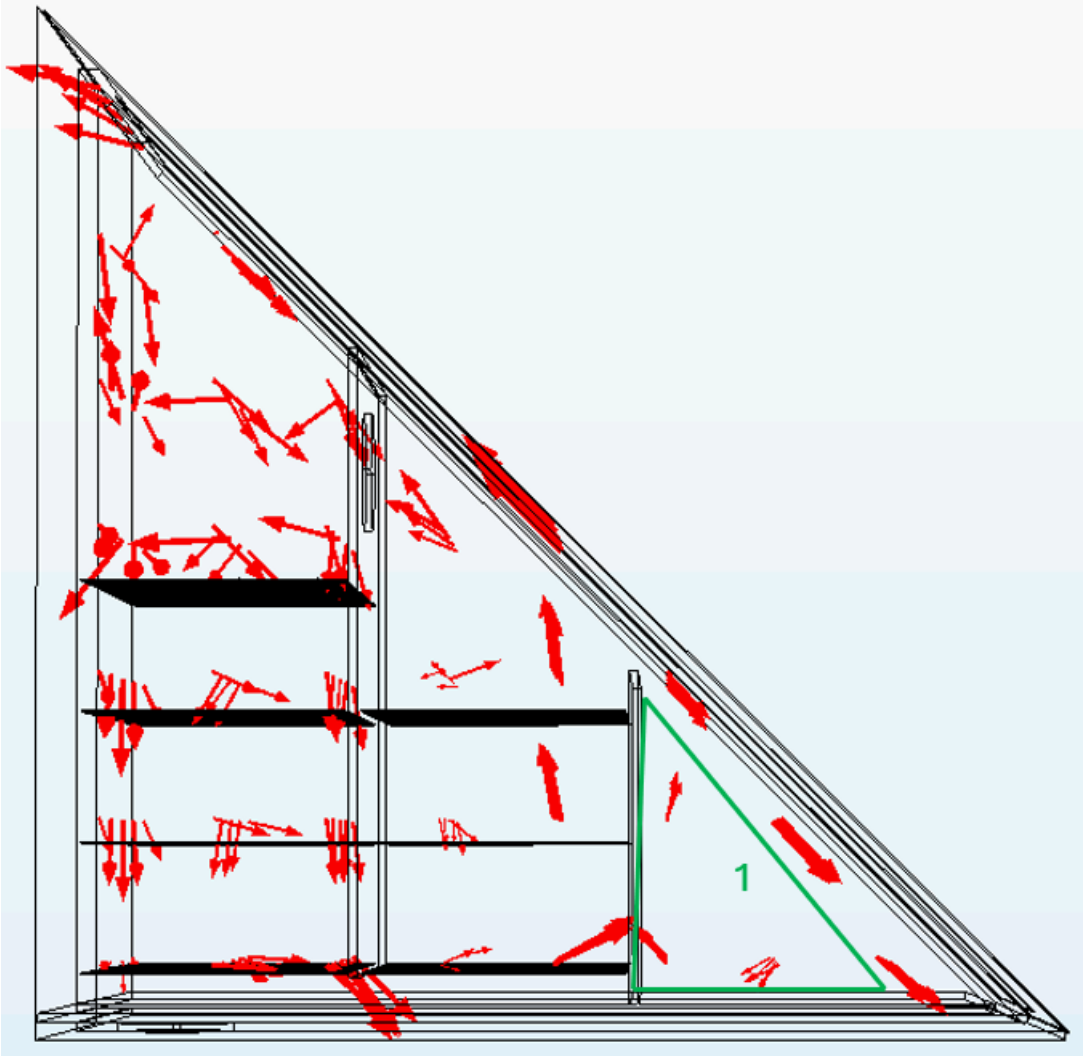

Figure 23: *Direction of the airflow inside the drying chamber. Internal fan and inlet fan size 120 mm, with a speed of 10 l/s. The distance between the shelves are 15 cm. The area marked with 1 shows the air vortex forming.*

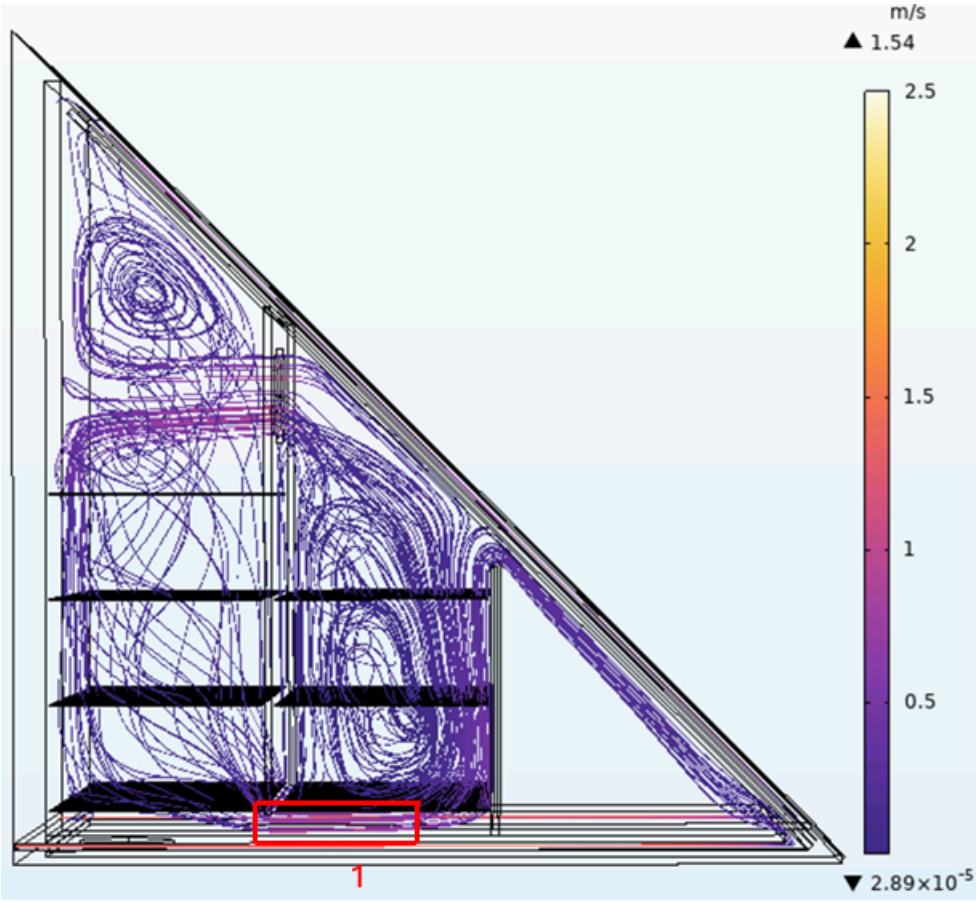

Figure 24: *The streamline of the airflow inside the air domain. The area marked with 1 shows the air picking up speed.*

4.3.2 Dryer with 7 shelves, 2 shelves with slices of apples on them

Adding cylinders with a radius of 2 cm on the two bottom shelves in the second drying chamber to represent slices of apples gave the same result as it did for the first design.

The vortex in the second drying chamber was decreased and confined between the two bottom shelves, as can be seen in the area marked with 2 in Figure 25. This could potentially lead to uneven drying on what is on the bottom shelf of the second drying chamber.

Also, this seems to lead to the vortex between the second drying chamber and the outlet increasing in size, as can be seen in the area marked with 3 in Figure 25. The average speed in the air volume is 0.16 m/s.

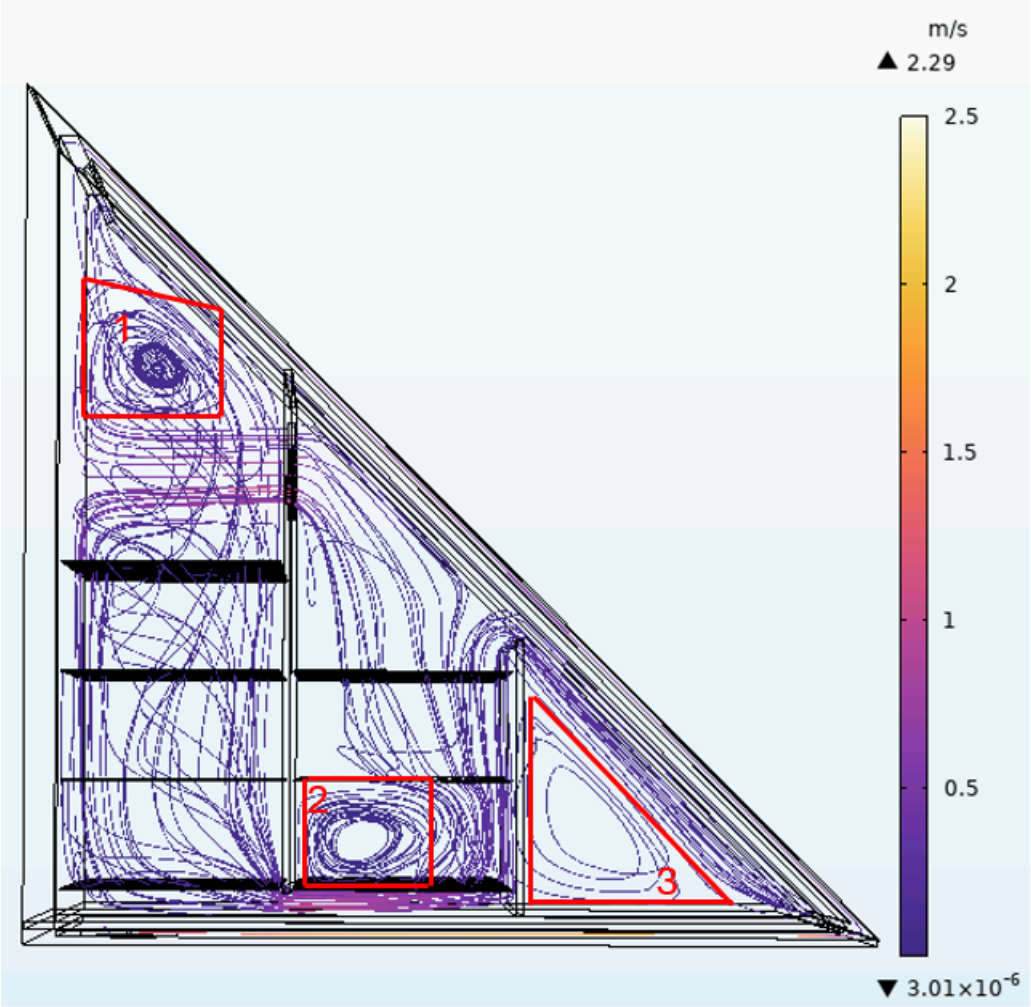

Figure 25: *The streamline of the airflow inside the air domain. The area marked with 1 shows the air vortex in chamber one and the area marked with 2 shows the air vortex in the second drying chamber. The area marked with 3 shows an air vortex forming.*

4.3.3 Second design with design changes

For the second design, the first parameter that was changed was to increase the size of entry gap to the drying chamber from 2 cm to 6 cm. This did not have the same positive effect as it had with the first design. The vortex in the first drying chamber seems to have decreased somewhat in size when comparing the area marked with 1 in Figure 26 with the area marked with 1 in Figure 25. An air vortex is still forming between the second drying chamber and the outlet, as can be seen in the area marked with 1 in Figure 27, and the small air vortex in the second drying chamber is still there, as can be seen in the area marked with 2 in Figure 25

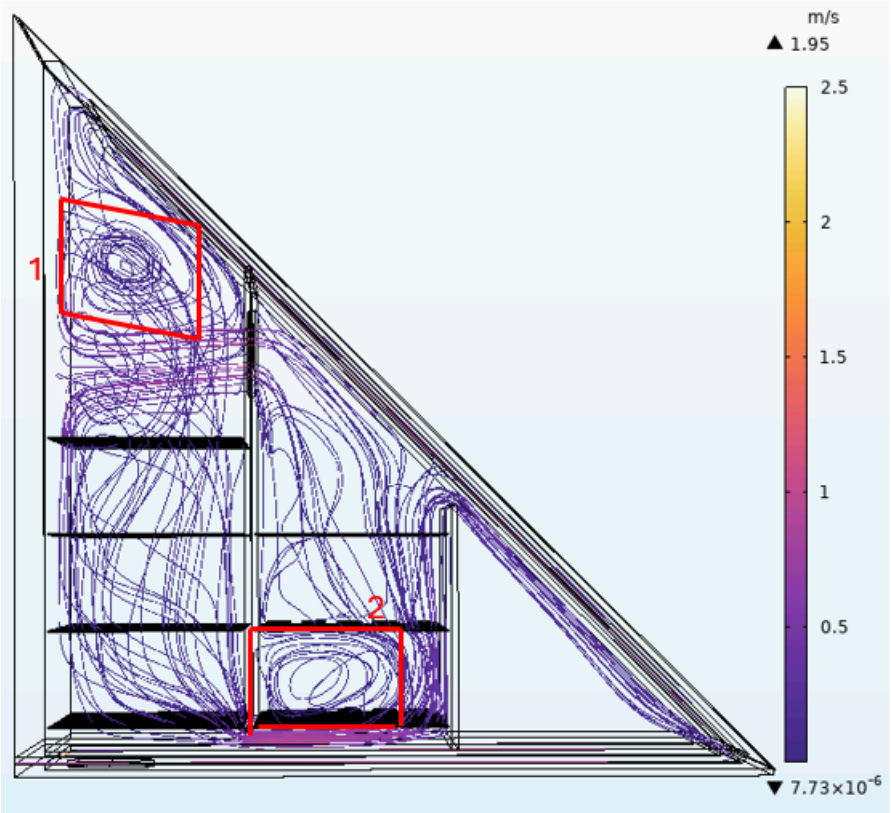

Figure 26: *The velocity of the airflow inside the air domain, with larger entry gap to the drying chamber. The area marked with 1 shows the air vortex in chamber one and the area marked with 2 shows the air vortex in the second drying chamber.*

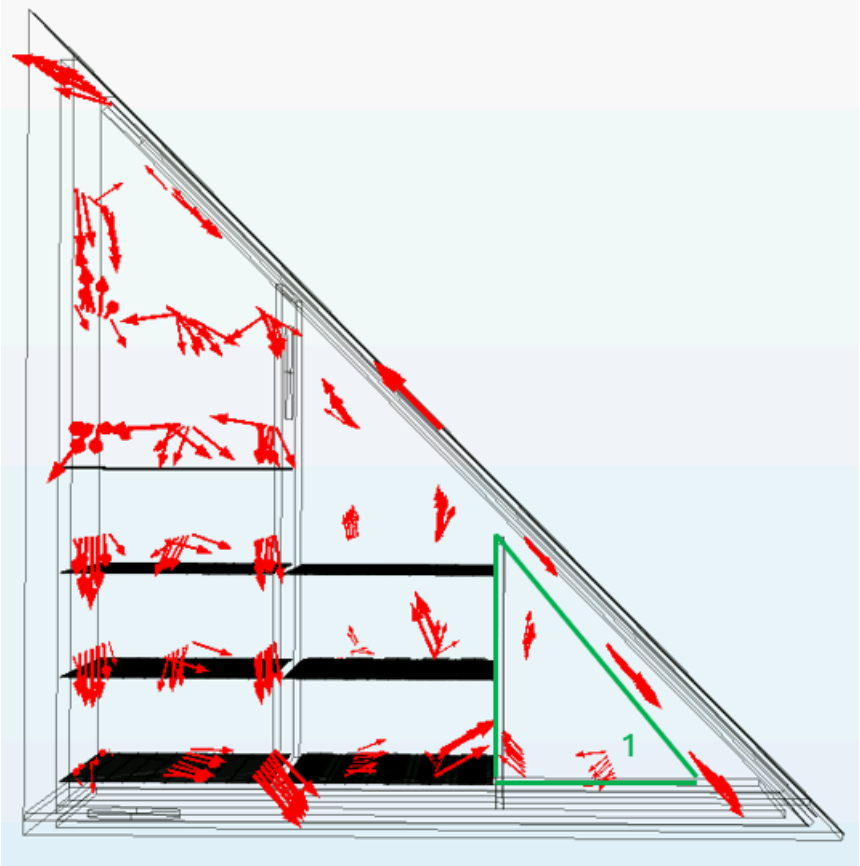

Figure 27: *Direction of the airflow inside the drying chamber, with larger entry gap to the drying chamber. The area marked with 1 shows the air vortex in the area between the second drying chamber and the outlet.*

The second change of parameter was to add a second internal fan, placing the two internal fans 26.5 cm from the end of the wall and 33 cm between the two fans. This seems to have some effect on the air vortex in the first drying chamber, but the vortex is still forming as can be seen in the area marked with 1 in Figure 28. Also, the vortex in the second drying chamber is still forming and appears unchanged, as can be seen in the area marked with 2 in Figure 28. Another result of adding a second internal fan is that some of the air is moving back from the outlet of the drying chamber to the second drying chamber instead of going out of the solar dryer, as can be seen in the area marked with 1 in Figure 29. This can have some effect on the heat exchanger since the air leaving the drying chamber is supposed to heat up the heat exchanger. Additionally, the vortex is still forming between the second drying chamber and the outlet, as can be seen in the area marked with 2 in Figure 29.

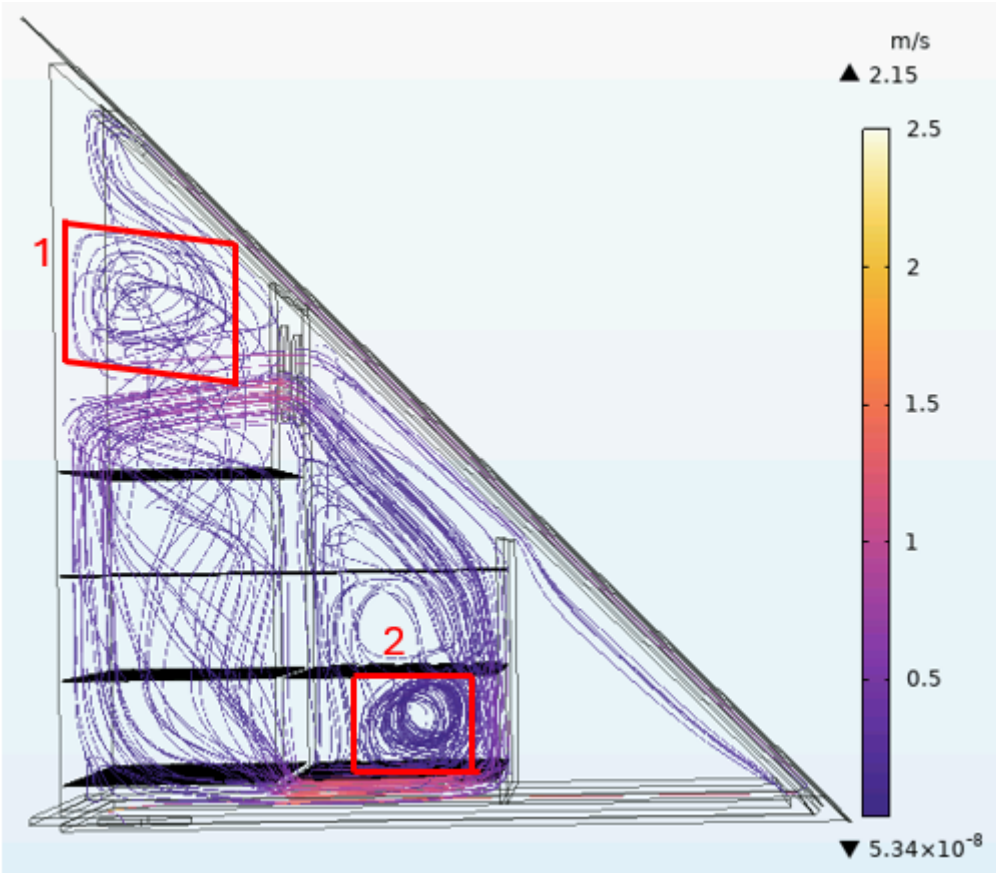

Figure 28: *The velocity of the airflow inside the air domain, with larger entry gap to the drying chamber and the two internal fan. The speed on the internal fans is 10 l/s. The area marked with 1 shows the air vortex in chamber one and the area marked with 2 shows the air vortex in the second drying chamber.*

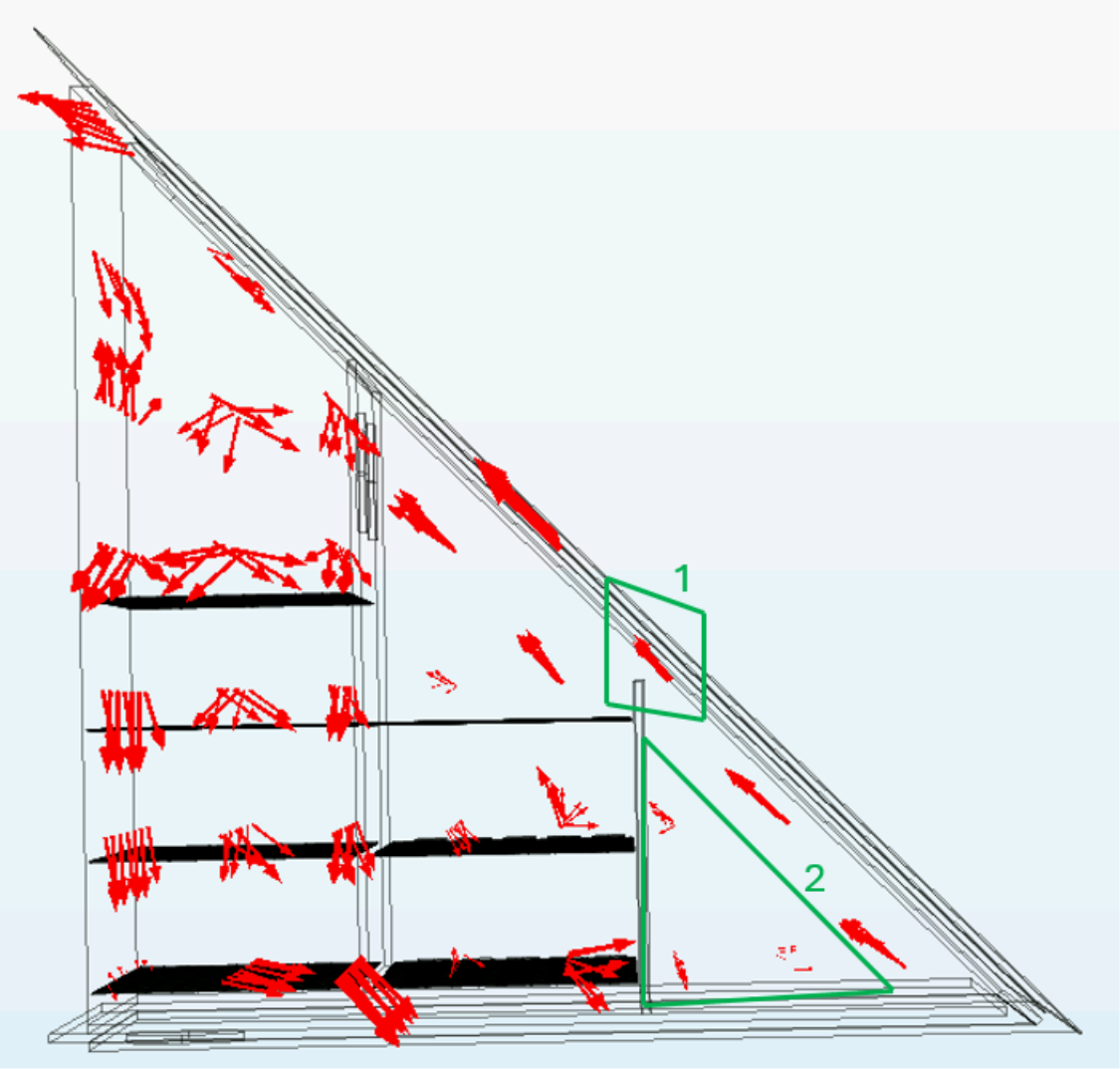

Figure 29: *Direction of the airflow inside the drying chamber,with larger entry gap to the drying chamber and the two internal fans. Internal fans and inlet fan have a size of size 140 mm and a speed of 10 l/s. The distance between the shelves is 15 cm. The area marked with 1 shows the air going back to the second drying chamber. The area marked with 2 shows the air vortex in the second drying chamber.*

In the last simulation a wooden board was added to block off the empty space between the second drying chamber and the outlet of the drying chamber, so air would not start building up a vortex. This eliminated the vortex forming between the second drying chamber and the outlet. However, the problem with air going back to the second drying chamber from the outlet still exists, as can be seen in the area marked with 1 in Figure 30. The vortex in the first drying chamber has decreased in size, but a vortex is still forming, as can be seen in the area marked with 1 in Figure 31. One thing that may be the cause of this is the steeper angle on the solar dryer, which is 45°compared to the 30°on the first design. This makes it harder to get a good airflow at the top of the first drying chamber. The vortex in the second drying chamber is still forming and does not seem to be affected by the changes, as can be seen in Figure 31. The average speed in the air volume for this design is 0.19 m/s.

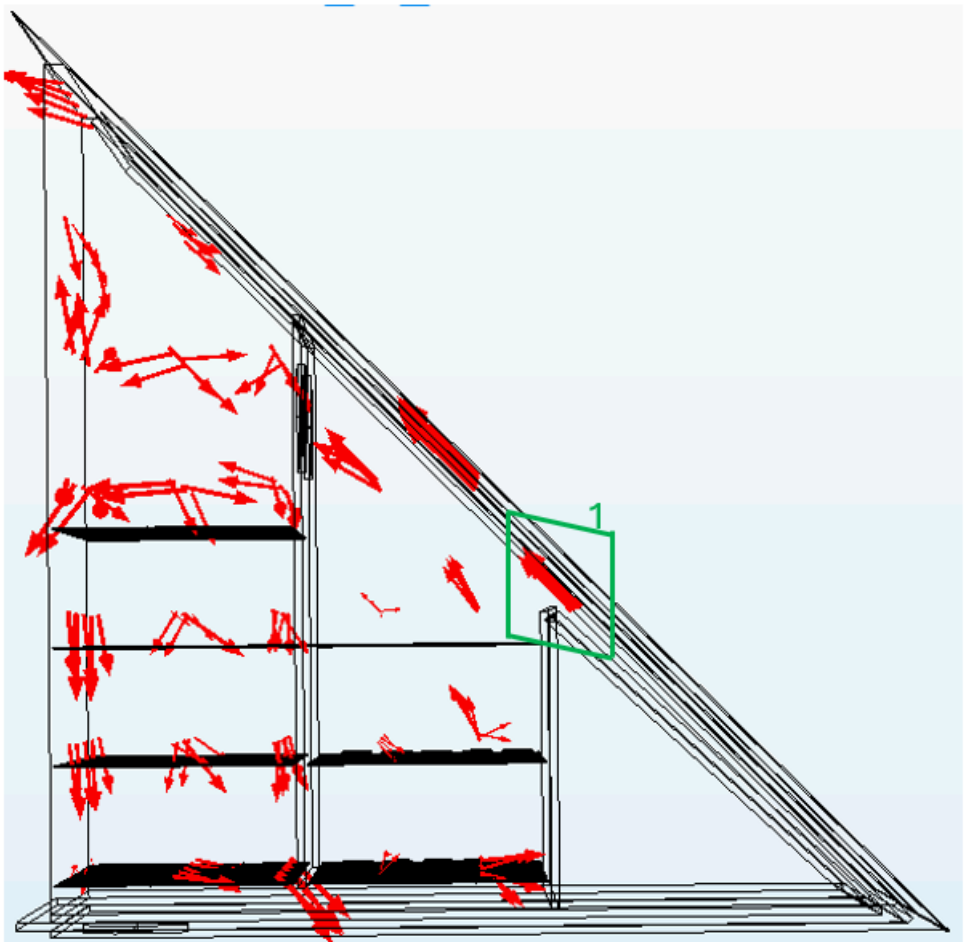

Figure 30: *Direction of the airflow inside the drying chamber, with a larger entry gap to the drying chamber, two internal fans and a wooden board to block of the empty space between the second drying chamber and the outlet of the drying chamber. The area marked with 1 shows the air going back to the second drying chamber.*

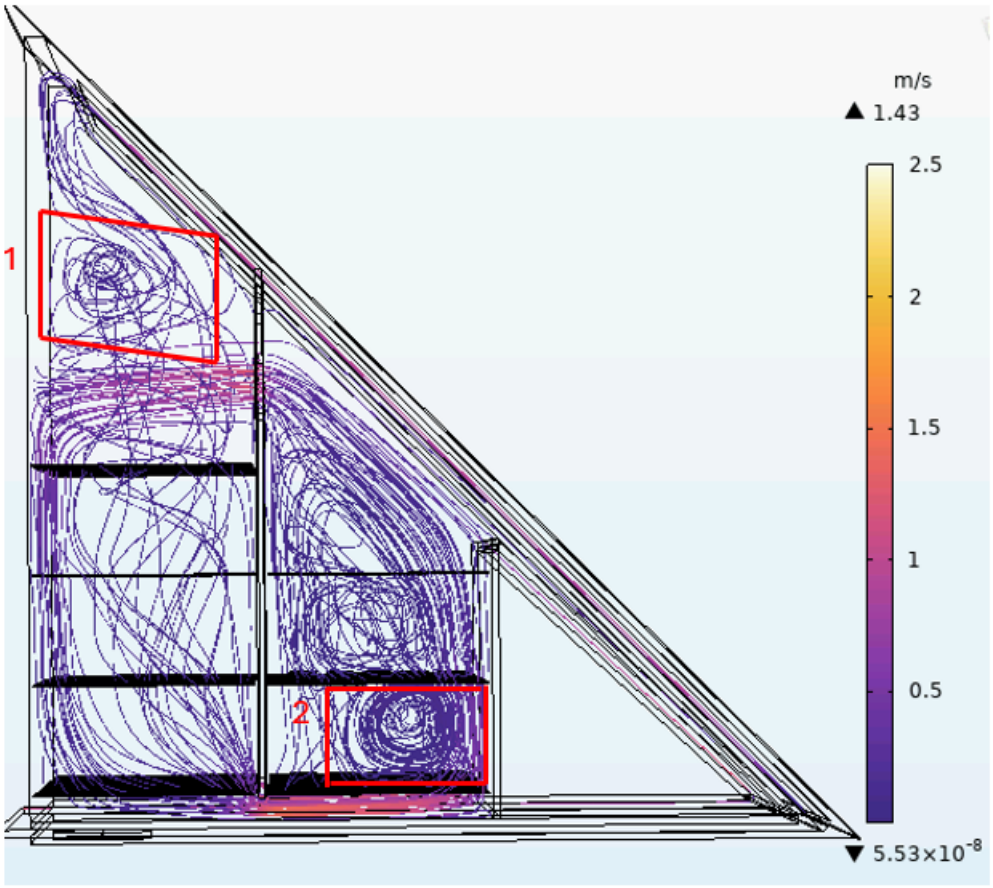

Figure 31: *The velocity of the airflow inside the air domain, with larger entry gap to the drying chamber, two internal fans and a wooden board to block of the empty space between the second drying chamber and the outlet of the drying chamber. The speed on the internal fans is 10 l/s. The area marked with 1 shows the air vortex in chamber one and the area marked with 2 shows the air vortex in the second drying chamber.*

4.4 Pressure

4.4.1 Comparing an empty dryer with 7 shelves with a dryer with 7 shelves where 2 shelves that have slices of apples on them

Comparing the pressure for the empty dryer with seven shelves with the pressure for when having two shelves with apples shows that there is almost no difference in pressure, as can be seen in Figure 32. The largest pressure drop for both setups occurs at the inlet of the dryer, as can be seen in the area inside the rectangles in Figure 32. For both configurations, the average pressure inside the air volume is 5.07 Pa.

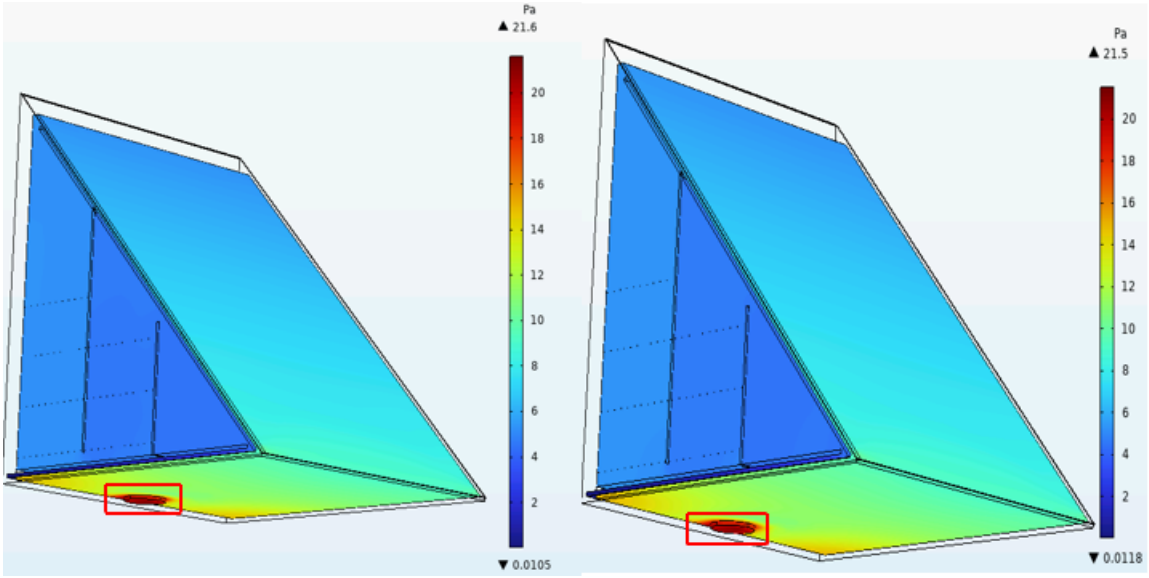

Figure 32: *The pressure in the air volume, to the left empty dryer with 7 shelves and to the right is 2 shelves with slices of apples on them. The area inside the red rectangles shows the largest pressure drop point. The area marked in both figures shows the largest pressure drop.*

4.4.2 Second design with design changes

Increasing the entry gap to the drying chamber has a very small effect on the pressure. When adding the one internal fan, the pressure inside the drying chamber becomes negative, as can be seen in Figure 33. The negative value can be explained by considering that atmospheric pressure is defined as zero at the inlet. Therefore, a negative pressure value within the solar dryer indicates that the pressure inside is lower than at the inlet. When adding the wooden board to block off the empty space between the second drying chamber and the outlet of the drying chamber, the pressure inside the air volume remains unchanged. The only difference is that the sealed-up space has a pressure of zero Pa, as can be seen in the area marked with 1 in Figure 34. The largest pressure drop still occurs at the inlet of the dryer, as can be seen in the area marked with 2 in Figure 34. This is optimal since this leads to an increase of the air velocity that should help the air to circulate through out the solar dryer. Also the fan does not need as much energy to operate as in the first design which means this design is more energy-efficient than the first design.

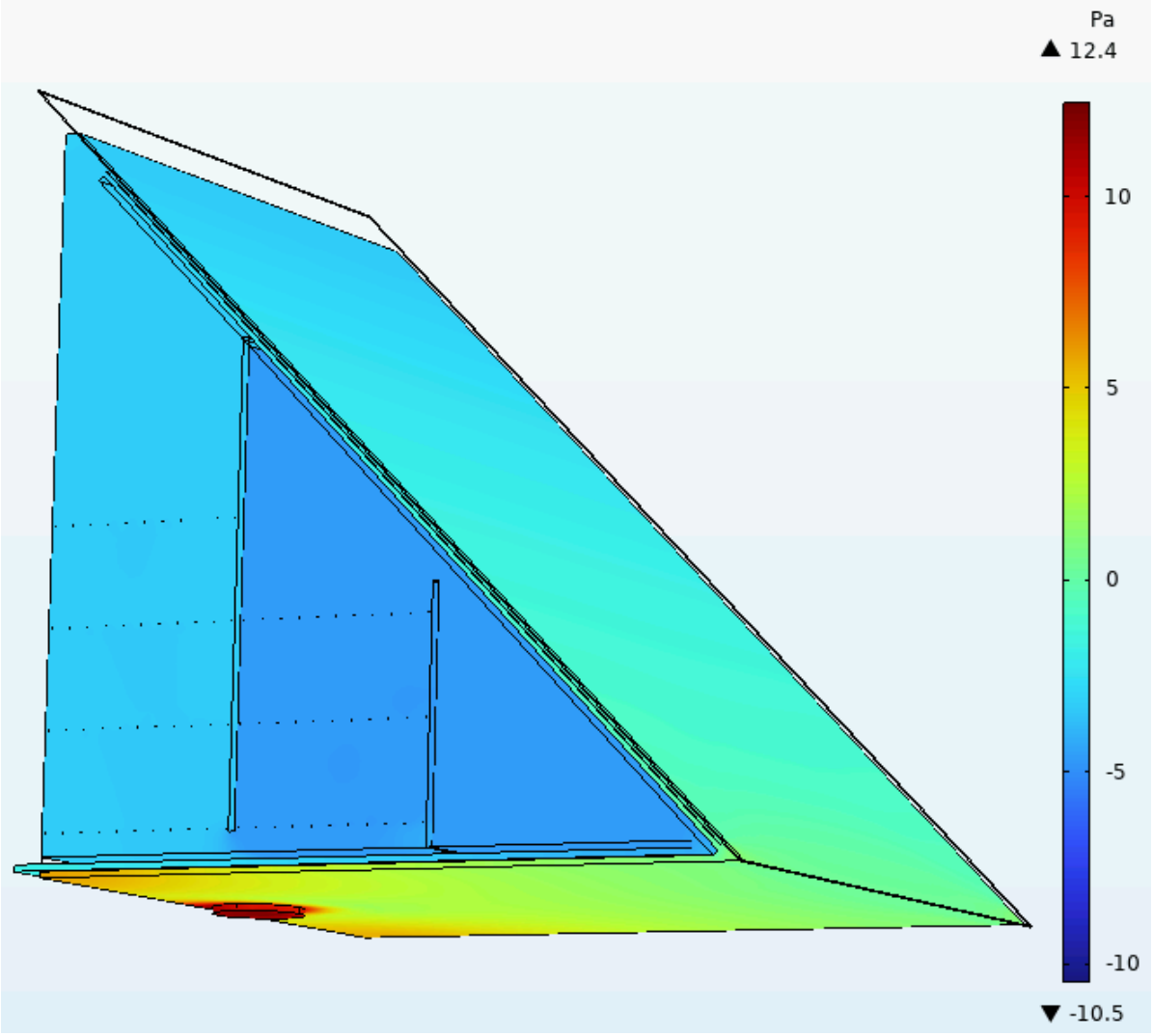

Figure 33: *The pressure inside the air volume, with larger entry gap to the drying chamber and the two internal fan. The size of internal fans and inlet fan is 140 mm, with a speed of 10 l/s.*

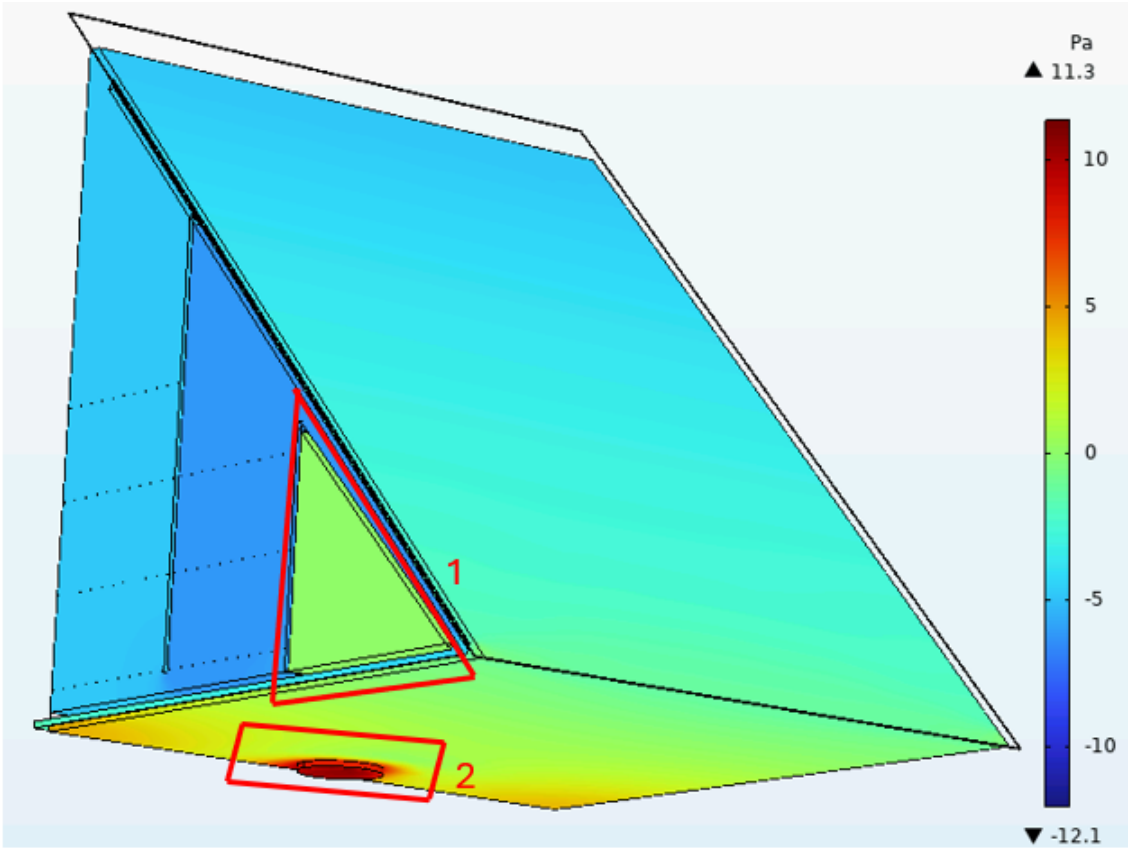

Figure 34: *The pressure inside the air volume, with larger entry gap to the drying chamber, the two internal fan and the wood board. The area marked with 1 shows the sealed off area. The area marked with 2 shows the largest pressure drop.*

4.5 A New Design

4.5.1 Improving the airflow in the drying chamber

Using the results from the simulations done on the first and second design, a new design of the solar dryer was developed. The aim with the new design was to address the issue of the air vortex in the second drying chamber. This was done by removing the centre panel, thus simplifying the solar dryer's construction. Moreover, the addition of a second internal fan at the bottom of the drying chamber aimed to enhance air circulation and compensate for the loss of the speed boost provided by the centre panel between the two drying chambers. The design is depicted in Figure 35.

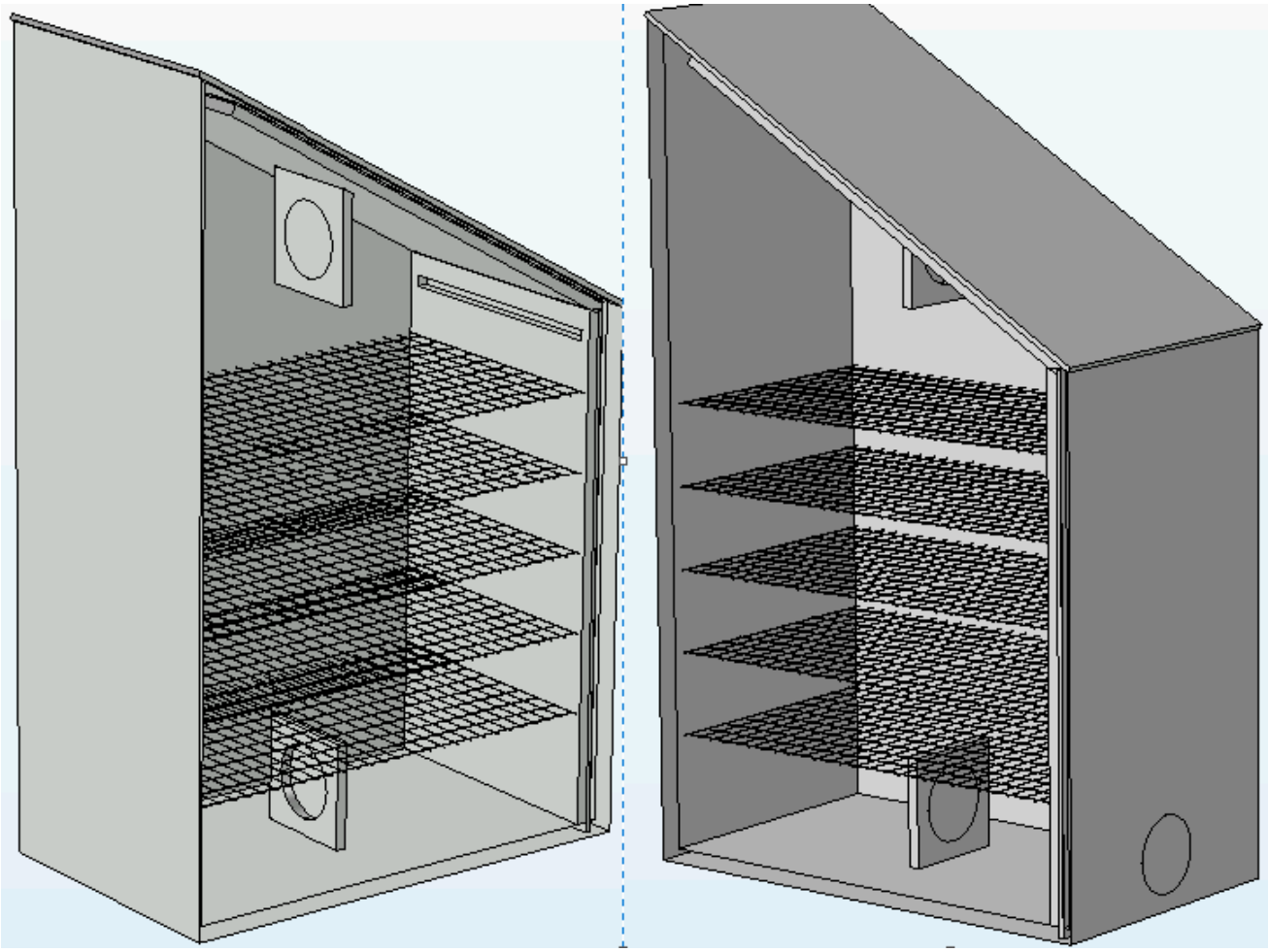

Figure 35: *Inside the solar dryer with one large drying chamber and two 140 mm internal fans.*

The result of this design was that the airflow appeared to shift more horizontally within the drying chamber as can be seen in the area marked with 1 in Figure 36 compared to the configuration shown in Figure 15. Additionally, an air vortex seemed to emerge in the upper back corner of the drying chamber, marked as 1 in Figure 37. At the bottom of the drying chamber, marked as 2 in Figure 37, the air moved back and forth in that area rather than predominantly upward in the chamber. The second internal fan aimed to improve air circulation in the drying chamber. However, it did not achieve the desired effect, as evident by the observed airflow pattern within the marked area with 2 in Figure 37. Furthermore, this design exhibited the same issue of air moving close to the back wall of the drying chamber, as depicted in Figure 37.

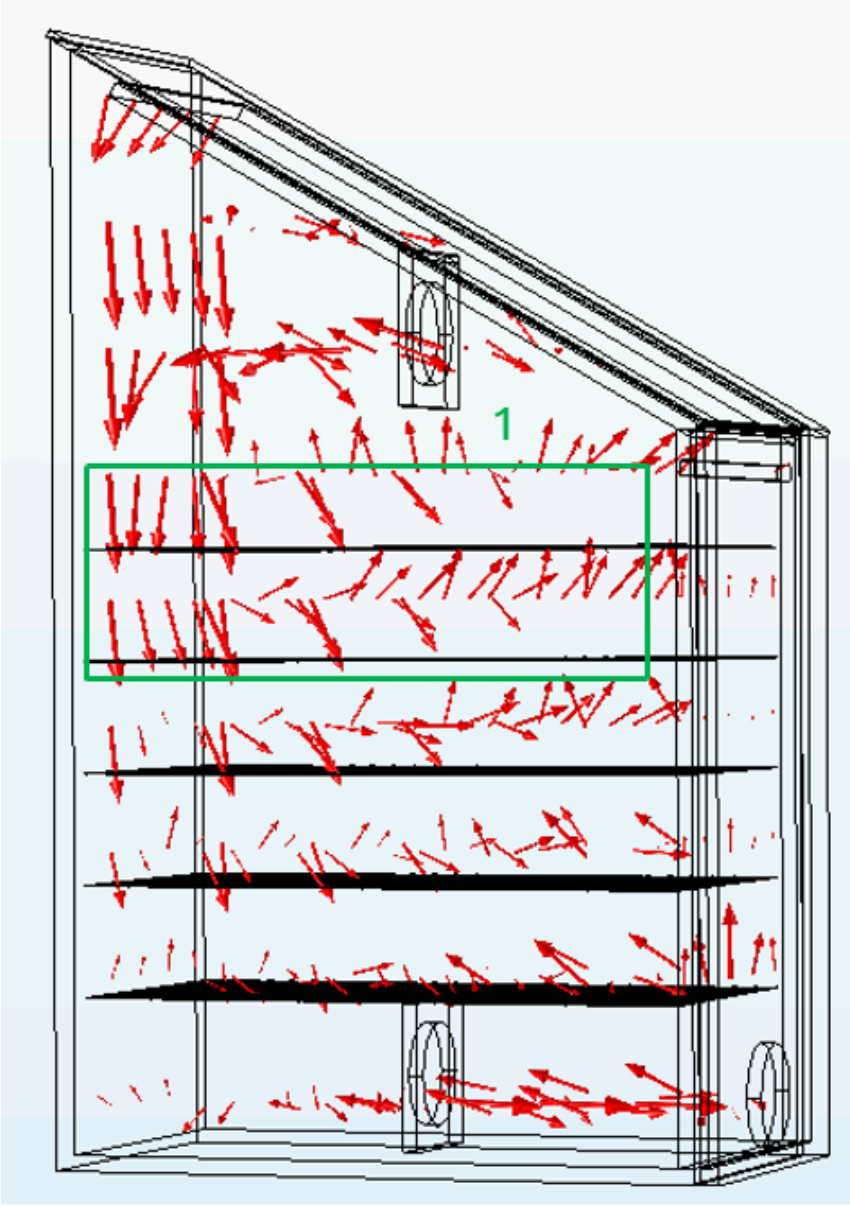

Figure 36: *Direction of the airflow inside the drying chamber. The area marked with 1 shows the air going horizontally within the drying chamber.*

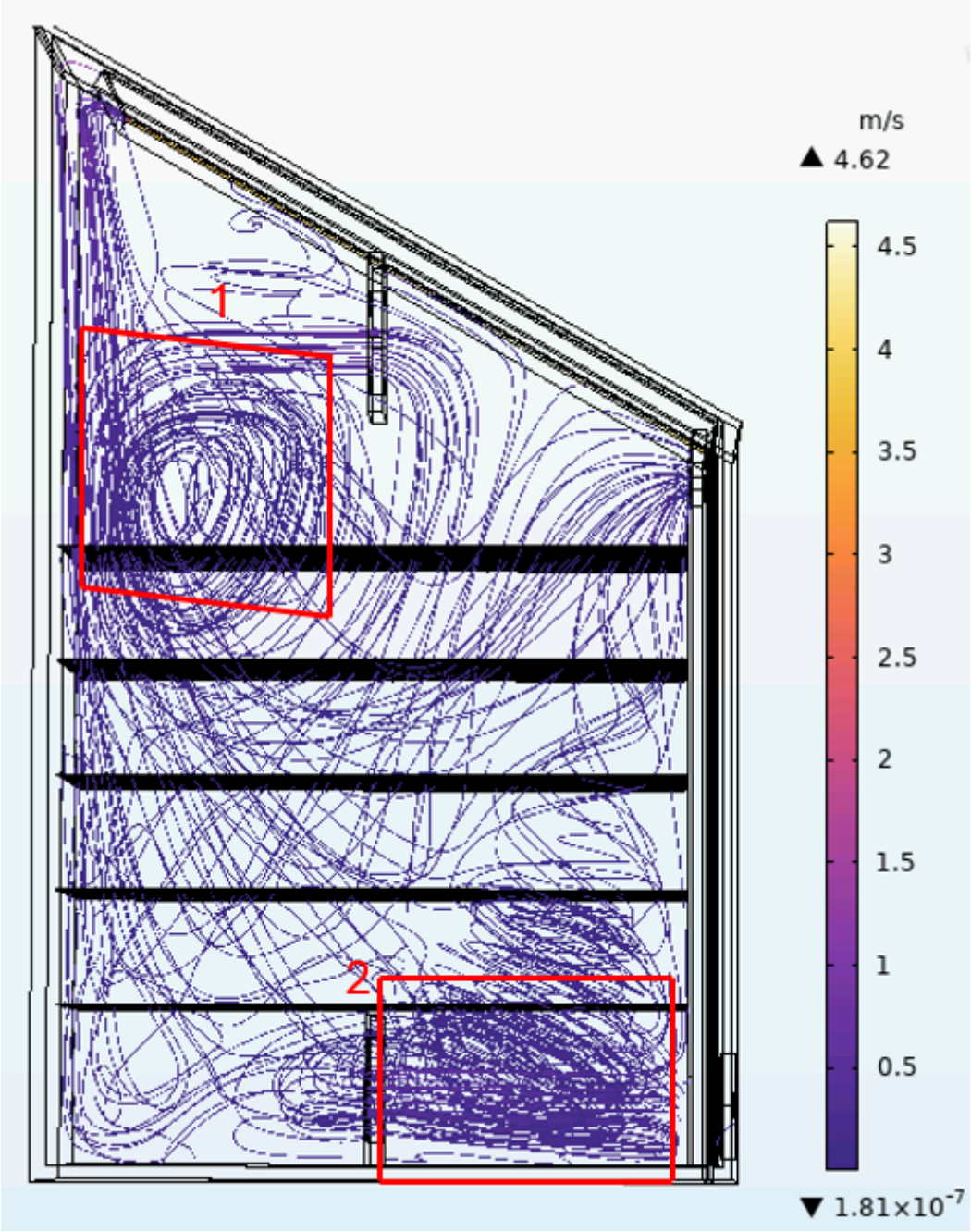

Figure 37: *The streamline of the airflow inside the air domain. The area marked with 1 shows the air vortex in upper part of the chamber and the area marked with 2 shows the air moved back and forth.*

4.5.2 Pressure

For the new design, the largest pressure drop still occurs when the air is reaching the absorber, as can be seen in the area marked with 1 in Figure 38. Also, the maximum pressure has increased to 141 Pa compared with 87.4 Pa that the first design had, while still maintaining the speed of the external fan at 10 l/s. The reason behind this could be that in the new design, the external fan is placed inside the front panel of the solar dryer, as can be seen in the area marked with 2 in Figure 38. However, the pressure drop at the inlet is still very small. It would be more optimal if the pressure drop resembled that of the second design, where the largest pressure drop occurs at the inlet.

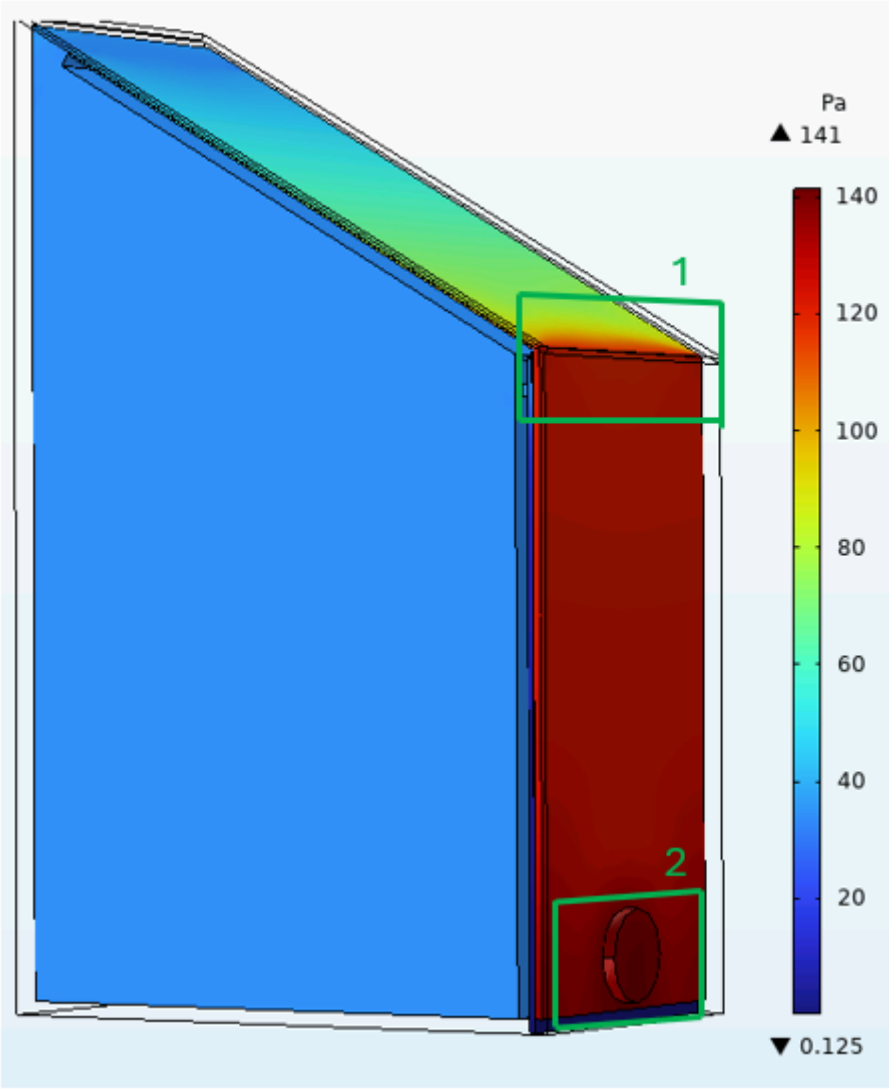

Figure 38: *The pressure inside the air volume.The area marked with 1 shows the largest pressure drop. The area marked with 2 shows the placement of external fan.*

5 Discussion

5.1 Airflow

The result for the first design suggests that the placement of the internal fan has a large impact on the air vortex that arises at the entry of the drying chamber. If the internal fan is placed too low, a portion of the air will be pushed up towards the entry, and in combination with a narrow entry to the drying chamber, this creates the air vortex. Placing the fan as high as possible on the wall that separates the two drying chambers and increasing the entry gap to the drying chamber leads to the air vortex decreasing by a large margin. This is something we want to strive for since the air coming into the drying chamber is the air that has been heated by the heat exchanger and absorber and should be pushed out into the drying chambers. Now it lingers at the top of the drying chamber and may not be optimal for the drying process and for the efficiency of the process. To get answers to these questions, experiments need to be conducted and compared with the results from those experiments. The vortex in the second drying chamber was not eliminated with these design changes, and it needs to be addressed. Having a vortex that covers a large portion of the bottom shelf in the second drying chamber may result in uneven drying of the crop in the solar dryer, and that is one problem that the Solar Food project is supposed to solve.

Regarding the second design, the problem with the air vortex at the top of the drying chamber is hard to solve. The angle of the solar dryer is so steep that the air from the internal fan will not reach the top of the chamber even if it is placed as high as possible on the wall that separates the two drying chambers. This means that to eliminate the vortex for this design would require more than adding a second internal fan and making the entry gap larger. Although these changes help decrease the size of the vortex, they won't make it disappear completely, as shown in Figure 31. Adding a second internal fan has an undesirable effect of making some of the air flow back to the second drying chamber instead of leaving through the outlet, as can be seen in the area marked with 1 in Figure 29, and due to lack of time, this problem was not solved.

Another observation regarding the flow for the two different designs is that much of the air in the first drying chamber flows close to the wall. This may not be optimal because the less air that passes over the fruit, the slower the drying process would be for the fruit. Another observation regarding the two different designs is the air vortex at the bottom shelf of the second drying chamber. The vortex seems to be a difficult problem to solve, and it can be an obstacle when it comes to getting the crop to dry evenly on the bottom shelf. Maybe this is the uneven drying that was observed during the experiments conducted on the second design by Jamtsho and Om (2023), but they do not specify where this uneven drying was observed.

What is mentioned in the paragraph above was the basis for the new design that was made on the solar dryer. The centre panel that divided the drying chamber into two separate chambers seems to be the source of the air vortex in the second drying chamber. Because of the increase in velocity by having the air move through the smaller space between the two drying chambers, it creates the air vortex in the second drying chamber. The idea was that by removing the centre panel, the problem with the air vortex in the second drying chamber would be solved, and making the construction of the solar dryer less complex. This was not the case; the vortex was gone but having one drying chamber led to the air moving more horizontally in the drying chamber than before. This raises the question: is it more efficient to have air moving vertically or horizontally over the product that is drying? This is beyond the scope of this project and it would need to be investigated by conducting experiments on the drying process in a laboratory. Also, in the third design, it seems that even more air moves along the wall than in the two other designs, and that is also an issue. An attempt to solve this issue was to have a ramp on the wall to try to direct the air out from the wall, as can be see on the following page in Figure 39. But due to time constraints, that design's simulation never went through, so whether this is a solution to the problem is unclear.

When it comes to the third design, no conclusions can be drawn since the third design has raised more questions than answers. For the first and the second design, the first design seems to have fewer problems to solve when it comes to the airflow. But since there are no calculations to confirm this, it needs more tests to determined which one of the two designs is the best one.

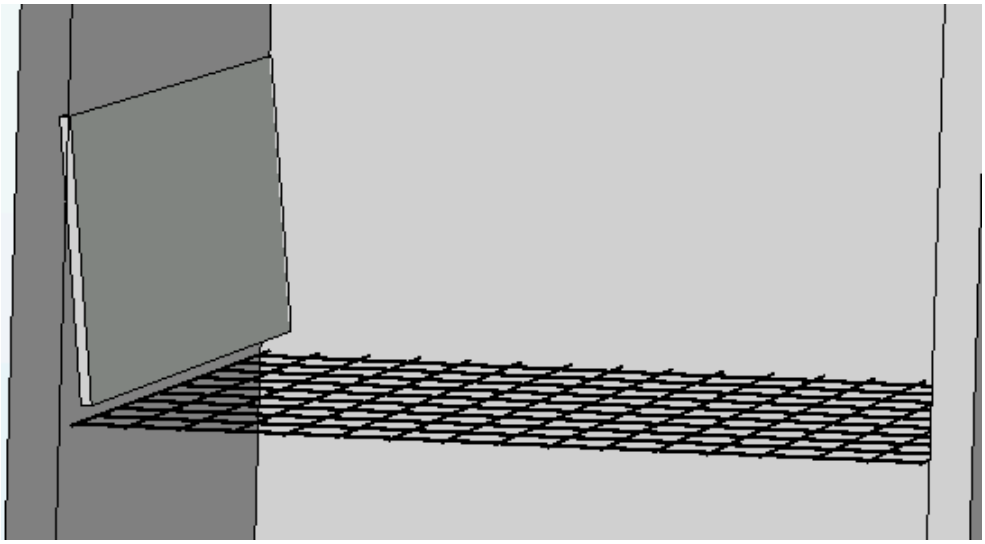

Figure 39: *Idea to force the air out from the wall. The shelf in the pitcure is the top shelf in the first drying chamber.*

5.2 Pressure

Comparing the different pressure drops in the first design with design changes to the new design, it becomes clear that having the external fan in the front panel of the dryer leads to a higher maximum pressure value, as can be seen in Figure 38 and in Figure 22. We know that fluid in a system will always flow from a region of higher pressure to a region of lower pressure or vice versa, and therefore a large difference in pressure should lead to a higher flow. Therefore, regardless of which design we decide to invest in, the external fan should be placed in the front panel of the solar dryer to provide better flow through the dryer, as shown in Figure 38.

When it comes to the pressure for the second design, the maximum pressure is much lower compared to the first design, and this is because the air volume in the second design is much larger than in the first design. The pressure loss in the second design is by a factor of four lower than in the first design, meaning that less energy is required to power the fan in the second design than in the first design. This makes the second design more energy-efficient than the first design and gives the desirable increase in the velocity of the air at the inlet of the solar dryer. In Figure 33, the pressure for the second design has a negative value inside the dryer, which means that the pressure inside the dryer is lower than the defined atmospheric pressure at the inlet. This means that if the atmospheric pressure outside the dryer is 100 Pa, the pressure inside the drying chamber in this case in Figure 33 is 97 Pa.

5.3 The Problem with Heat Transfer

In the start of this project, the goal was to examine both the airflow and the heat transfer from both the heat exchanger and the absorber. However, the heat transfer was not functioning correctly. The desired effect was that the air leaving the drying chamber would be heated up by the heat exchanger, and the heat exchanger should increase the temperature of the incoming air by 8-12 °C, but it only heated up the air by 3 °C. After a discussion with the supervisor, it was decided that due to time constraints, the project's focus would shift to improving the airflow of the solar dryer since that aspect was working in the simulations. This means that the numbers presented in this work are not entirely accurate and should be interpreted with caution, as temperature affects both airflow and pressure.

5.4 Limitations of the Simulations

The goal from the start of the project was to get the element size of the mesh to be as small as possible. But when time became an issue, that idea had to be changed since the simulation on the larger element size took between 15-20 hours per simulation. This also led to limitations when it came to simulating different speeds on the fans for the existing designs, and the speed on the external fan was kept at 10 l/s. Both Rissler (2023), Jamtsho, and Om (2023) all had come to the conclusion that it was the optimal velocity for the heat exchanger and absorber.

When it came to heat storage the decision was made not to include heat storage on the advice of the supervisor. Since the efficiency of having heat storage had been questioned by both Rissler (2023), Jamtsho, and Om (2023).

6 Conclusion

The conclusions that can be drawn from the simulations in this project, is that the two designs have similar issues when it comes to the airflow. The issues were that air vortexes formed in the two drying chambers in both designs where the second design even has a third air vortex forming between the second drying chamber and the outlet. Another issue was that alot of the air flows along the back wall in the first drying chamber. These issues can affect the drying process of the crop, especially the air vortex in the second drying chamber can lead to uneven drying of the crop on the lower shelf.

The adjustments that were made to these two designs in this project and during the simulations were as follows; for the first design, the entry gap to the drying chamber was made larger, and the internal fan was moved higher up. These adjustments were done in an attempt to improve the air vortex issue and the adjustments did remove the air vortex in the first drying chamber. But the issues with the air vortex in the second drying chamber and the air along the wall, were not affected by these adjustments and remained unsolved.

For the second design the adjustments included making the entry gap larger to the drying chamber, adding a second internal fan, and adding a wooden board to seal off the area between the second drying chamber and the outlet. These adjustments had no effect on the issues with the air vortex in the first drying chamber, the air vortex in the second drying chamber and with the issue of the air moving along the back wall and these were not solved during this project.

The new design presented in this project had the goal to solve the issue with the air vortex in the second drying chamber, by removing the centre panel. The air vortex was not forming anymore, but the issue of the air moving along the wall was still present. With the new design other issues arose such as air moving more horizontally than before in the drying chamber and the air moving back and forth in the bottom of the drying chamber rather than predominantly upward in the chamber.

6.1 Future Work

In future work, it would be necessary to solve the issues with air flowing along the wall in the first drying chamber and the air vortex in the second drying chamber to ensure that the solar dryer dries the products evenly.

Additionally, future work could involve getting the heat transfer to function properly and enabling simulation of the solar dryer regardless of design in COMSOL. This would be an important contribution to allow testing and running of different setups.

References

Briney, A. (2018). *Winds and the pressure gradient force.* Retrieved 2024-01-17, from https://www.thoughtco.com/winds-and-the-pressure-gradient-force-1434440

Britannica. (2023). *Turbelent flow.* Retrieved 2024-01-19, from https://www.britannica.com/science/turbulent-flow

Chhogyel, N., & el al. (2018). *Climate change and potential impacts on agriculture in bhutan: a discussion of pertinent issues.* Retrieved 2023-11-06, from https://agricultureandfoodsecurity.biomedcentral.com/articles/10.1186/s40066-018-0229-6

Comsol. (2022a). *Comsol multiphysics® simulation software.* Retrieved 2023-10-04, from https://doc.comsol.com/5.4/doc/com.comsol.help.cfd/IntroductionToCFDModule.pdf

Comsol. (2022b). *Comsol multiphysics® simulation software.* Retrieved 2023-10-06, from https://doc.comsol.com/6.1/doc/com.comsol.help.heat/IntroductionToHeatTransferModule.pdf

Comsol. (2023a). *About comsol.* Retrieved 2024-01-19, from https://www.comsol.com/company

Comsol. (2023b). *Importance of meshing and how to build the mesh.* Retrieved 2024-02-08, from https://www.comsol.com/video-training/getting-started/building-the-mesh-for-a-model-geometry-in-comsol-multiphysics

Comsol. (2023c). *Introduction to heat transfer module.* Retrieved 2023-10-18, from https://www.comsol.com/comsol-multiphysics

Comsol. (2023). *The laminar flow interface.* Retrieved 2024-01-17, from https://doc.comsol.com/5.5/doc/com.comsol.help.cfd/cfd_ug_fluidflow_single.06.008.html

Desrosier, N. W., & Singh, R. P. (2024). *Food preservation.* Retrieved 2024-03-01, from https://www.britannica.com/topic/food-preservation

Ganji, D. D., & el al. (2017). *Nonlinear heat transfer: Mathematical modeling and analytical methods.* Amsterdam: Elsevier.

Jamtsho, T., & Om, D. (2023). *Design, analysis and performance evaluation of indirect solar dryer* [Master's thesis, Lund University]. (Available at https://lup.lub.lu.se/student-papers/search/publication/9141281)

Karan, P., et al. (2023). *Bhutan.* Retrieved 2023-10-18, from https://www.britannica.com/place/Bhutan

Ndawula, J. (2023). *Alterations in fruit and vegetable beta;-carotene and vitamin c content caused by open-sun drying, visqueen-covered and polyethylene-covered solar-dryers.* Retrieved 2024-02-27, from https://www.ajol.info/index.php/ahs/article/view/6873

Probert, A. (2022). *Development and testing of a novel solar dryer design with an incorporated heat exchanger - for use in the himalayan regions* [Master's thesis, Lund University]. (Available at https://lup.lub.lu.se/student-papers/search/publication/9085862)

Rissler, C. (2023). *Mitigating post-harvest losses in bhutan through solar food drying: Optimization and analysis* [Master's thesis, Lund University]. (Available at https://lup.lub.lu.se/student-papers/search/publication/9124967)

Shahidian, & el al. (2020). *Bio-engineering approaches to cancer diagnosis and treatment.* Academic

Press.

Simscale. (2023a). *What is heat transfer?* Retrieved 2023-12-25, from https://www.simscale.com/docs/simwiki/heat-transfer-thermal-analysis/what-is-heat-transfer/

Simscale. (2023b). *What is laminar flow.* Retrieved 2024-01-17, from https://www.simscale.com/docs/simwiki/cfd-computational-fluid-dynamics/what-is-laminar-flow/

Simscale. (2023c). *What is turbelent flow.* Retrieved 2024-01-19, from https://www.simscale.com/docs/simwiki/cfd-computational-fluid-dynamics/what-is-turbulent-flow/

Sokolova, I. (2019). *Encyclopedia of ecology (second edition).* Retrieved 2023-12-26, from https://www.sciencedirect.com/topics/earth-and-planetary-sciences/convective-heat-transfer

Streeter, V. L. (1961). *Fluid mechanics.* McGraw Hill.

The Engineering ToolBox. (2003a). *Conductive heat transfer.* Retrieved 2023-12-29, from https://www.engineeringtoolbox.com/conductive-heat-transfer-d_428.html

The Engineering ToolBox. (2003b). *Conective heat transfer.* Retrieved 2024-01-25, from https://www.engineeringtoolbox.com/conductive-heat-transfer-d_428.html

The Engineering ToolBox. (2003c). *The ideal gas law.* Retrieved 2024-01-22, from https://www.engineeringtoolbox.com/ideal-gas-law-d_157.html#gsc.tab=0

The Engineering ToolBox. (2003d). *Radiation heat transfer.* Retrieved 2024-01-25, from https://www.engineeringtoolbox.com/radiation-heat-transfer-d_431.html

The Engineering ToolBox. (2003e). *Reynolds number.* Retrieved 2024-01-17, from https://www.engineeringtoolbox.com/reynolds-number-d_237.html

The World Bank. (2017). *World bank partners with bhutan to improve agriculture productivity and food security for bhutanese people.* Retrieved 2023-10-19, from https://www.worldbank.org/en/news/press-release/2017/09/21/partner-with-bhutan-improve-agriculture-productivity-food-security

The World Bank. (2023). *The world bank in bhutan.* Retrieved 2023-10-19, from https://www.worldbank.org/en/country/bhutan/overview#1

WFP. (2020). *Wfp's support to nutrition in bhutan.* Retrieved 2024-02-27, from https://reliefweb.int/report/bhutan/wfp-s-support-nutrition-bhutan